# Cement Composition and Structural Durability in Florida

**Final Report**

**Prepared for**

**Florida Department of Transportation**

**State Project Number BC353 - 29**

**October 2003**

**Dr. A. Zayed**

**zayed@eng.usf.edu**

**Department of Civil and Environmental Engineering**

**University of South Florida**

**4202 E Fowler Avenue**

**Tampa, FL 33620**

# ACKNOWLEDGEMENT

This work has been supported by the Florida Department of Transportation. The principal investigator appreciates the technical assistance offered by Mr. M. Bergin, PE., Technical Project Manager during the course of this investigation.

## Disclaimer

**Technical Report Documentation Page**

| 1. Report No. | 2. Government Accession No. | 3. Recipient's Catalog No. |
|---|---|---|
| 4. Title and Subtitle<br>**Cement Composition and Structural Durability in Florida** | | 5. Report Date<br>October 2003<br>6. Performing Organization Code |
| 7. Author(s)<br>**Dr. Abla Zayed, Ph.D.**<br>**Natalya Shanahan, Kurt Brown and Amin Hanhan** | | 8. Performing Organization Report No. |
| 9. Performing Organization Name and Address<br>**Department of Civil and Environmental Engineering**<br>**University of South Florida**<br>**4202 E. Fowler Avenue; ENB 118**<br>**Tampa;FL 33620-5350** | | 10. Work Unit No. (TRAIS)<br>11. Contract or Grant No.<br>BC353-29 |
| 12. Sponsoring Agency Name and Address<br>**Florida Department of Transportation**<br>**605 Suwannee St. MS 30**<br>**Tallahassee, Florida 32399**<br>**(850)414-4615** | | 13. Type of Report and Period Covered<br>**Final Report**<br>14. Sponsoring Agency Code |

15. Supplementary Notes

**Prepared in cooperation with the USDOT and FHWA**

16. Abstract

**This study was initiated to address the need to adhere to a maximum limit on tricalcium silicate content in cements used in the State of Florida. Several cements with variable tricalcium silicate content (48%- 67%- Bogue) were selected for this study. Cement characterization included: morphology of clinker, particle fineness, particle size distribution, oxide chemical analysis, phase content determination using x-ray diffraction. Durability studies on mortar prepared with as-received cements included: strength in lime and sodium sulfate solution and expansion measurements on mortar bars exposed to sulfate solution. In addition, mortar cubes and bars prepared with cements doped with tricalcium silicate, were studied for strength variation and expansion in sodium sulfate solution. Concrete mixes were prepared to assess the strength variation in sulfates, chloride ingress through RCP measurements and open-circuit potential measurements. Phase transformation accompanying failure was determined through x-ray diffraction. The results indicate that for cements with similar tricalcium aluminate content, increasing tricalcium silicate content of cements above 57% results in an increase in deterioration as assessed by strength drop and expansion in sodium sulfate solutions. For cements with high tricalcium silicate content, the drop in strength and the increase in expansion experienced by mortar at 120 days of exposure to sodium sulfate solution were 1,500 psi and 2% respectively. The deterioration was accompanied by abundance in ettringite and gypsum. Based on the results of this research it is recommended that for durable concrete exposed to a sulfate environment, maximum limit on tricalcium silicate content in cements has to be in effect.**

| 17. Key Word | 18. Distribution Statement |
|---|---|
| **alite, sulfate durability, x-ray diffraction, morphology of clinker phases, ettringite, gypsum, hemihydrate, anhydrite, tricalcium silicate limit, tricalcium aluminate content** | **No Restriction**<br>**This report is available to the public through the NTIS, Springfield, VA 22161** |

| 19. Security Classif. (of this report) | 20. Security Classif. (of this page) | 21. No. of Pages | 22. Price |
|---|---|---|---|
| **Unclassified** | **Unclassified** | | |

# EXECUTIVE SUMMARY

## Introduction

The objective of this investigation was to determine the effect of tricalcium silicate on the short and long term durability of concrete. Towards satisfying the above objective, several approved Florida Department of Transportation [FDOT] cement suppliers were contacted for material collection. Four cements and their matching clinkers were used in this study. The selected cements shared similar fineness but variable tricalcium silicate content. Since the selected cements had variable phase content, additions of laboratory-prepared tricalcium silicate was used in order to eliminate any concerns that can be generated from variations in the other cement phases' contents.

The as-received material was subjected to several characterization tests that include mineralogical x-ray diffraction for cement phases quantification. Two techniques were used, internal standard method and Rietveld refinement. Oxide chemical composition of the as-received cements was determined by x-ray fluorescence. Cement particle morphology was studied through Blaine fineness, particle size distribution, and optical microscopy of the clinker. Mortar cubes and bars were exposed to a sodium sulfate environment to assess sulfate durability. Mortar cubes were monitored for strength variation and mortar bars were prepared for expansion measurements. In addition, concrete mixes were prepared for all cements to assess the effects of tricalcium silicate content on concrete durability. Strength, RCP and open-circuit potential (OCP) measurements were conducted on the concrete specimens. At the end of the reported period of this investigation, scanning electron microscopy and x-ray diffraction studies were performed in order to determine the phase transformation accompanying deterioration.

## Results and Recommendations

The findings of this study indicate that there is a need to maintain limits for a maximum tricalcium silicate content for better sulfate durability. The determined phase

composition through Bogue calculations might not reflect that proper phase content. X-ray diffraction was found to be a valuable tool in determining the actual phase content. The two methods used to determine tricalcium silicate content in cements were in agreement and supported the physical changes in mortar and concrete specimens. In addition, it was found that increasing tricalcium silicate content, for cements exposed to sulfate environments, had a significant effect on strength. Cements with high tricalcium silicate content (of 60% and above) experienced a drop of approximately 1000 psi at an age of 180 days. For higher tricalcium silicate content (69%), the drop in strength observed at 120 days was about 1,500 psi. Expansion measurements indicated a dependence of the amount of expansion on the tricalcium silicate content of the cements. Cements with tricalcium silicate with 60% expanded at a faster rate than lower tricalcium silicate cements (57%). Higher $C_3S$ cements experienced an average expansion of 1% at 330 days while lower $C_3S$ cements had a corresponding expansion of 0.18% at the same age. RCP results were indicative of a strong dependence on the $C_3S$ content. At an age of 120 days, only concrete that was made with high tricalcium silicate content has experienced a strength drop. Scanning microscopy and x-ray diffraction studies indicate that increasing the tricalcium silicate increased the abundance of expansive ettringite and gypsum. Since the findings of this study indicate that increasing tricalcium silicate content accelerated the rate of deterioration, it is recommended that a limit on the maximum allowable tricalcium silicate content has to be enforced.

# CHAPTER 1I

# LITERATURE REVIEW

.

The major compounds formed in the clinker are tricalcium silicate ($Ca_3SiO_5$), dicalcium silicate ($Ca_2SiO_4$), tricalcium aluminate ($Ca_3Al_6O_{12}$), and tetracalcium aluminoferrite ($Ca_4Al_8Fe_8O_{28}$). The short-hand notation for these compounds used in cement industry is $C_3S$, $C_2S$, $C_3A$, and $C_4AF$ respectively. $C_3S$ is responsible for early strength development, setting and hardening of concrete; $C_2S$ determines later strength development, $C_3A$ controls heat evolution during hydration, and $C_4AF$ is for sulfate resistance.

$C_3S$ forms when calcium oxide combines with silica; it crystallizes from clinker liquid at about 1450°C. $C_3S$ has several polymorphs with three different crystal structures: triclinic, monoclinic, and rhombohedral. In pure $C_3S$, the triclinic form exists up to 980°C, which at this temperature converts to monoclinic, which in turn converts to rhombohedral when temperature exceeds 1070°C. Therefore, pure compound cooled to room temperature, should be in the triclinic form. However, the presence of such substitution ions as $Mg^{2+}$, $Al^{3+}$ or $Fe^{3+}$ can cause the higher temperature polymorphs to remain, even when clinker is cooled to room temperature [1-4]*. In cement, $C_3S$ is most frequently observed in the monoclinic form [1].

$C_2S$ also has several polymorphs that have hexagonal, orthorhombic, and monoclinic structures. $\beta$-$C_2S$ and $\gamma$-$C_2S$, which are respectively monoclinic and orthorhombic, can exist up to 670°C at normal pressure. Up to 1160°C, orthorhombic $\alpha'_L$-$C_2S$ is present. Above that temperature, dicalcium silicate can exist either in the form of $\alpha'_H$- $C_2S$, which is orthorhombic, or $\alpha$-$C_2S$, which is hexagonal. The form of $C_2S$ that is most commonly present in clinker is $\beta$-$C_2S$ [4].

$C_3A$ polymorphs are cubic ($\beta$-$C_3A$), orthorhombic ($\alpha$-$C_3A$), and monoclinic; $C_4AF$ does not have any polymorphs [4]. $C_4AF$ is present in the clinker as a solid solution series that approximates the composition of brownmillerite ($4CaO{\cdot}Al_2O_3{\cdot}Fe_2O_3$) [1].

* Numbers in brackets refer to the references at the end of the report

Reaction of cement with water is called hydration. Cement hydration consists of a series of complex chemical reaction that proceed at the same time. Alite reacts with water to form amorphous calcium silicate hydrate gel and calcium hydroxide, also called portlandite. The abbreviated notation for these compounds is C-S-H and CH.

$$3CaO{\cdot}SiO_2 + (3 + m - n)H_2O \rightarrow \quad (1)$$

$$nCaO{\cdot}\ SiO_2{\cdot}mH_2O + (3 - n)Ca(OH)_2$$

Reaction of belite with water is very similar to that of alite, only it proceeds at a slower rate. The reaction products of belite hydration are also C-S-H and CH.

Tricalcium aluminate reacts with calcium sulfate and water to form ettringite. The reaction can be expressed as follows:

$$3CaO{\cdot}Al_2O_3 + 3CaSO_4{\cdot}2H_2O + 26H_2O \rightarrow \quad (2)$$

$$3CaO{\cdot}Al_2O_3{\cdot}3CaSO_4{\cdot}32H_2O$$

If $C_3A$ is more reactive than calcium sulfate, it will form calcium aluminate monosulfate hydrate according to reaction (3) or calcium aluminate hydrate according to reaction (4), depending on the differences in reactivity.

$$2(3CaO{\cdot}Al_2O_3) + 3CaO{\cdot}Al_2O_3{\cdot}3CaSO_4{\cdot}32H_2O + 4H_2O \rightarrow \quad (3)$$

$$3(3CaO{\cdot}Al_2O_3{\cdot}CaSO_4{\cdot}12H_2O)$$

$$3CaO{\cdot}Al_2O_3 + Ca(OH)_2 + 12H_2O \rightarrow 4CaO{\cdot}Al_2O_3{\cdot}13H_2O \quad (4)$$

Reaction (3) can also take place if the supply of sulfate ions is exhausted before all the $C_3A$ has hydrated [1].

The hydration reaction of tetracalcium aluminoferrite yields products very similar to those produced during $C_3A$ hydration. Generally, the $C_4AF$ reaction rate is slower, although its reactivity depends on its exact chemical composition and Fe/Al ratio [1].
The mechanism of ettringite formation and its relationship to concrete sulfate durability has occupied researchers for the past 40 years. Although the exact mechanism of

ettringite formation is not known, many researchers speculate that ettringite is formed topochemically or by a through-solution mechanism. Topochemical reactions are defined as reactions that *"form a true crystalline overgrowth on the reactant with matching d-spaces … in the space occupied by the reactant."* However, the strict definition of topochemical reactions is rarely used in cement chemistry. Rather, any reaction during which *"the reaction product precipitates only within the space that became available by the dissolution process or in its immediate vicinity"* is considered to be topochemical. In through-solution reactions products are transported away from the reactants and precipitate from solution at random [5]. The particular mechanism of ettringite formation is determined by the hydroxyl ion concentration in the pore solution. Lime and alkalies are a source of $OH^-$ [6] as well as CH produced during the hydration of calcium silicates. Presumably, formation of ettringite proceeds as a through-solution reaction at lime concentrations up to 0.020 M and as a topochemical reaction at higher concentrations [6]. An increase in the $OH^-$ ion concentration forces ettringite to deposit on top of the $C_3A$ grains as the solution becomes supersaturated with respect to ettringite [6]. Many researchers support the theory that it is the topochemical ettringite that causes expansion and not the through-solution ettringite [5,6].

High hydroxyl ion concentrations also have an effect on the size of ettringite [7,8]. Ettringite crystals formed in the absence of lime are at least 6 times longer and twice as thick as those formed in the presence of lime after 24 hours [8]. In the absence of lime, ettringite precipitates throughout the sample, forming long needle-like crystals arranged in rosettes and spherulites in cavities and *"compacted bundles"* of prismatic crystals on top of the $C_3A$ grains. This random formation of ettringite is characteristic of a through-solution mechanism. Addition of lime decreases the size of the formed ettringite [8].

Sodium oxide decreases the rate of initial $C_3A$ hydration as well as the rate of gypsum consumption. Potassium hydroxide, on the other hand, accelerates both of these processes as well as increases the transformation rate of ettringite to monosulfoaluminate [9]. The presence of alkali sulfates does seem to affect the rate of $C_3A$ hydration, but it does increase gypsum consumption and ettringite to monosulfoaluminate transformation. Also, a decreased compressive strength is usually associated with the presence of alkali

sulfates in cement [10]. The presence of alkalies in cement does not seem to have a significant effect on $C_3S$ reactivity [9,10].

Sulfate attack is one of the most typical chemical attacks on concrete. Sulfate attack usually occurs when concrete structures are exposed to seawater, groundwater, and rainwater containing sulfate ions. Although the literature on the causes of concrete expansion due to sulfate attack is inconclusive, formation of gypsum and ettringite are generally held responsible for expansion and subsequent deterioration of concrete during sulfate attack [11]. Secondary ettringite forms at the early stages of sulfate attack and is responsible for initial expansion. Gypsum begins to form at later stages of attack after both aluminate and sulfo-aluminate hydrates have been converted to ettringite. Formation of gypsum is an expansive reaction as well [12].

Sulfate ions diffuse through the cracks and pores in concrete and react with monosulfoaluminate to form ettringite.

$$4CaO{\cdot}Al_2O_3{\cdot}12H_2O + 2CaSO_4{\cdot}2H_2O + 16H_2O \rightarrow$$

$$3CaO{\cdot}Al_2O_3{\cdot}3CaSO_4{\cdot}32H_2O$$

This reaction results in a volume increase that creates internal stresses in the concrete matrix. These internal stresses lead to cracking and spalling of concrete, accelerating the rate of sulfate attack by providing an easier passage for the sulfate ions into the interior of the concrete [13]. Another expansive reaction that takes place is a reaction between sulfate ions and calcium hydroxide that results in formation of gypsum.

$$Ca(OH)_2 + SO_4^{2-}\,(aq) \leftrightarrow CaSO_4{\cdot}2H_2O + 2OH^-\,(aq)$$

Mindess believes that this reaction becomes significant only when sulfate ion concentrations reach above 1000 ppm. When sulfate ion concentration is between 1000 ppm and 4000 ppm, gypsum formation is secondary to the ettringite formation in terms of the driving force of concrete expansion. However, above 4000 ppm, gypsum formation becomes the primary expansive reaction [13].

The microstructure of the mortars subjected to sulfate attack can be characterized by three zones: a surface zone that is highly cracked and disintegrated, a zone of

deposition of gypsum and ettringite, and an interior zone that is free from attack products, but exhibits microcracks. Gypsum in the second zone is usually observed in the pores and in the transition zone, while ettringite is deposited throughout the paste [14].

Recently, Tian and Cohen [15] studied expansion of alite and alite plus silica fume pastes exposed to 5 % sodium sulfate solution. Alite was chosen to eliminate ettringite formation in the samples. All samples were cured in saturated lime solution up to 14 days, and then placed in sodium sulfate solution. All specimens showed no expansion for approximately 360 days. After that period, alite paste specimens exhibited high rate of expansion, reaching 0.1% expansion by 480 days. At the same time, samples containing silica fume showed no expansion. After 480 days of curing, x-ray diffraction was performed to determine the solid phases present in the samples. The analysis indicated gypsum as the main product formed. More gypsum was present in the samples without silica fume; there was also some unhydrated $C_3S$ in all the samples. The researchers concluded that gypsum formation causes expansion in alite pastes and that expansion can be significantly reduced by silica fume additions.

Tian and Cohen [16] also studied pastes prepared with two types of $C_3S$: one type (alite) consisted of monoclinic crystals with some impurities, and the other type was pure triclinic $C_3S$. Alite paste samples with and without silica fume (10 % replacement) were stored in 5 % sodium sulfate solution. Up to about 360 days, the specimens did not experience any significant expansion. After 360 days, samples without silica fume started to expand at a high rate reaching 0.1 % at 480 days. Samples with silica fume did not expand. $C_3S$ mortar samples had a dormant period of about 40 days. After that, they started to expand at a higher rate than alite samples. Samples without silica fume expanded by 1.05 % at 230 days. Samples containing silica fume only expanded by 0.04%. Alite specimens stored in ammonium sulfate solution expanded much more rapidly, reaching 1.28 % expansion at 60 days. There was no data for alite samples with silica fume or $C_3S$ for ammonium sulfate solution.

X-ray diffraction analysis showed that gypsum was the main phase formed in all the specimens. However, samples without silica fume had more gypsum than those with silica fume. The 11.6˚ peak of gypsum seemed to be higher in alite paste at 440 days than in the $C_3S$ paste at 220 days, even though the $C_3S$ paste had much higher expansion.

Alite samples cured in ammonium sulfate also showed high CH peaks. The conclusion of the study was that although the mechanism of gypsum formation in concretes exposed to sulfate attack is unclear, the formation of gypsum is expansive and causes distress.

Irassar et al. [16] evaluated the performance of two Type V cements with different $C_3S$ content (40 % and 74 %) in a pH-controlled sulfate environment (0.352 M $Na_2SO_4$). High $C_3S$ cement also had a high $C_3S$/ $C_2S$ ratio and a $C_3A$ content of 1 %. The $C_3A$ content of low $C_3S$ cement was zero.

The researchers [16] measured expansion, sulfate consumption, flexural and compressive strengths of the mortars prepared with these cements as well as their blends with 10 % and 20 % limestone filler (85 % $CaCO_3$) replacement and 20 % and 40 % natural pozzolana replacement. It was concluded that high $C_3S$ cement had poor resistance to sulfate attack. Cement with high $C_3S$ content experienced a 0.350 % expansion at 360 days, which was ten times greater than that of the low $C_3S$ cement (0.035 %). Addition of limestone filler increased expansion of both cements, whereas addition of pozzolanic material reduced expansion. Sulfate consumption was higher for high $C_3S$ cement. Addition of the limestone filler increased sulfate consumption for both cements, and addition of pozzolana either decreased it or had no significant effect on sulfate consumption.

There was no reduction in flexural strength observed for low $C_3S$ cement. Flexural strength of high $C_3S$ cement started to decrease after 180 days. 10 % limestone filler addition did not have a significant effect on flexural strength of either cement. However, flexural strength of both cements with 20 % filler started to decrease after 28 days. Mortars containing pozzolanic material gained strength up to 90 days; after 90 days, no significant change was observed. Compressive strength of the low $C_3S$ cement mortars was higher than that of the high $C_3S$ cement mortars. Addition of pozzolana improved compressive strength, while addition of limestone filler lead to strength loss.

X-ray diffraction analysis revealed the presence of relatively small gypsum peaks in the low $C_3S$ cement mortar, but no ettringite peaks were observed. Gypsum and secondary ettringite were found in high $C_3S$ cement mortars. Irassar et al. suggest that secondary ettringite in the high $C_3S$ cement mortar formed due to interaction between sulfate ions and ferroaluminate hydrates.

The researchers attribute the differences in durability of the two cements to their different $C_3S$ / $C_2S$ ratios. The increase in this ratio leads to the increased production of CH, which reacts with sulfate ions to produce gypsum. Irassar et al. do not specify the source of the sulfate ions; it is assumed that they are supplied by the sulfate solution. Based on the behavior of the low $C_3S$ cement, researchers conclude that gypsum causes expansion only after a certain percentage of it has formed. High gypsum content in mortar also provides a favorable environment for formation of expansive secondary ettringite. Since the high $C_3S$ cement had no $C_3A$, the ettringite that was observed by XRD was produced by the hydration of ferroaluminates. Although the researchers do not reflect on the mechanisms of these reactions, they state that high amounts of calcium hydroxide are responsible for the poor performance of the high $C_3S$ cement [16].

In an earlier paper, Gonzalez and Irassar observed that in mortars prepared with high $C_3S$ cements (60 % and 74 %) and no $C_3A$, gypsum precipitated in massive deposits in the air voids and in the transition zone around the aggregates. They attributed this phenomenon to higher quantities of CH in the transition zone and its higher porosity. The researchers believe that the deposition of gypsum in the transition zone was the cause of high expansion of these two mortars. Gonzalez and Irassar believe that once gypsum filled all the available voids in the C-S-H gel around the aggregates, the growing gypsum crystals started to apply crystallization pressure on the C-S-H gel, producing cracks in the structure. The authors suggest that after a certain amount of gypsum forms and it becomes a dominant phase, C-S-H gel loses cohesion, and expansive ettringite starts to form.

Mortars with low $C_3S$ content (40 % and 50 %) did not experience high expansion. These samples had less gypsum and gypsum crystals were of smaller size and dispersed throughout the paste [17].

Cao et al. investigated resistance to sulfate attack of Portland cements with similar fineness and different chemical compositions. They discovered that cement with low $C_3S$ (39%) and low $C_3A$ content (4.6%) had the best performance in sulfate environments. It exhibited the lowest compressive strength drop and lowest expansion. The strength reduction for all other cements was very similar. Cement with the highest C3A content (6.6%) had the highest expansion, although its $C_3S$ content was moderate

(51 %). It was observed under the SEM, that in the cements with higher $C_3S$ content gypsum tended to form in large veins that were parallel to the surfaces exposed to sulfate solution. However, in the low $C_3S$ cement gypsum was located throughout the sample. Ettringite was found in all cements. The authors concluded that lowering the $C_3S$ and $C_3A$ content of cement improves its resistance to sulfate attack [18].

The literature does indicate the significance of tricalcium aluminate on the sulfate durability of concrete. In addition, there is a clear limit, in all national standards, to the maximum allowed tricalcium aluminate content in cements, if used in environments where sulfate durability is of concern. However, no such agreement seems to exist for tricalcium silicate content.

# CHAPTER III

# Testing Program, Results and Discussion

## 3.1 Characteristics of As-Received Cements

As mentioned previously, this study was initiated in order to address adherence to setting a maximum limit on tricalcium silicate content of cements. To that effect, several Portland cements were selected with the primary objective of having a variable tricalcium silicate content. Four ASTM Type I cements were used in this study. In this section, materials characterization of the as-received cements will be presented.

### 3.1.1 Blaine Fineness

Fineness is an important parameter in determining the reactivity of cement. This is due to the fact that an increase in particles' fineness corresponds to an increase in the total surface area in contact with water during cement hydration. Based on these considerations, it was decided to eliminate fineness as a variable in this study. Therefore, all the cements in this study were specifically chosen to have similar fineness. Table 1 lists the values obtained for the Blaine fineness of the as-received cements. Based on these values, it can be concluded that all cements included in this study had similar fineness.

**Table 1. Blaine Fineness**

| Cement | CC | DD2 | EE | PP |
|---|---|---|---|---|
| Blaine Fineness ($cm^2/g$) | 3840 | 3880 | 3800 | 3820 |

### 3.1.2 Particle Size Distribution

Cements displaying similar fineness might have different particle size distribution. While fineness is an important parameter, particle size distribution is also critical to the rate of hydration. Figures 1 through 5 display the particle size distribution expressed as cumulative percent passing as well as individual percent retained for each cement. Malvern Mastersizer laser particle size analyzer was used for data collection. The data depicted in Figure -1 shows that though the cements had similar Blaine fineness, they have different particle size distribution. The as-received cements can be divided into two groups; that is, EE-PP and CC-DD2. Both CC and DD2 showed similar content for particles less than 10 microns (approximately 51-55%) while cements EE and PP had lower particle content passing the 10 microns size (approximately 40%). Based on the individual percent-retained graphs, CC has a mode particle size of 10-microns, DD2 cement has a mode particle size of 15 microns, and EE and PP cements have the mode particles size of approximately 20 microns.

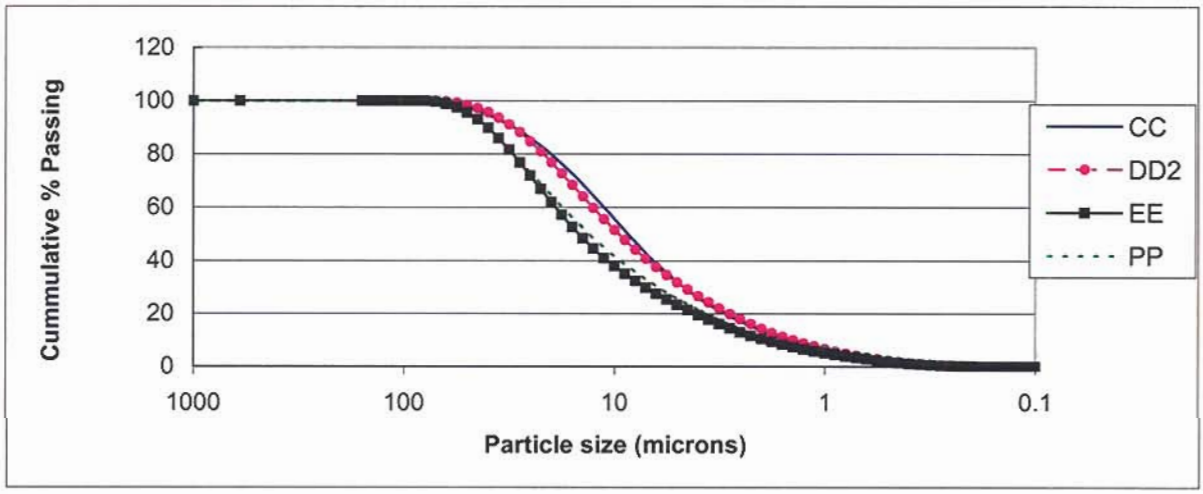


**Figure 1. Particle Size Distribution for As-received Cements**

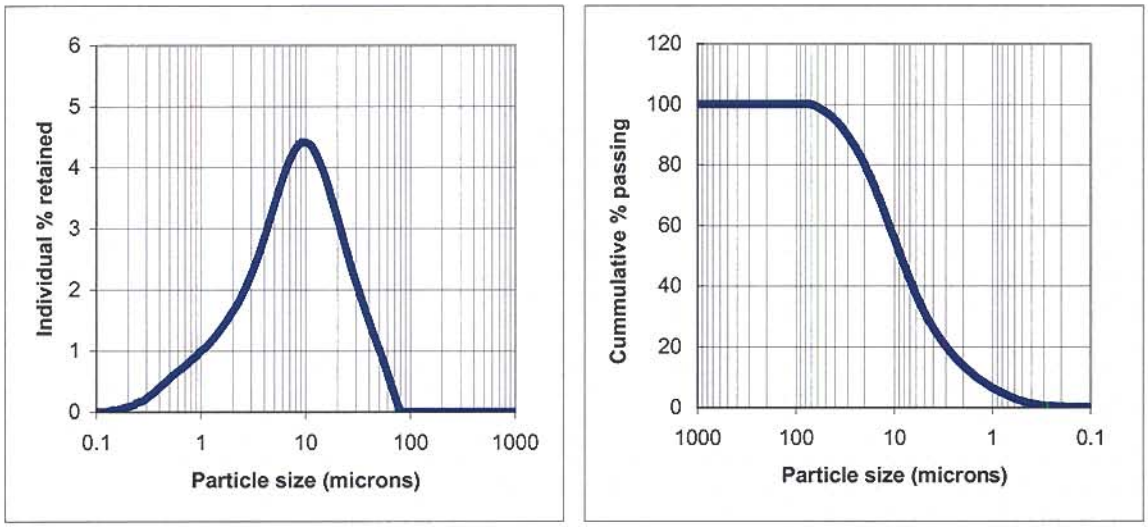


**Figure 2. Particle Size Distribution for Cement CC**

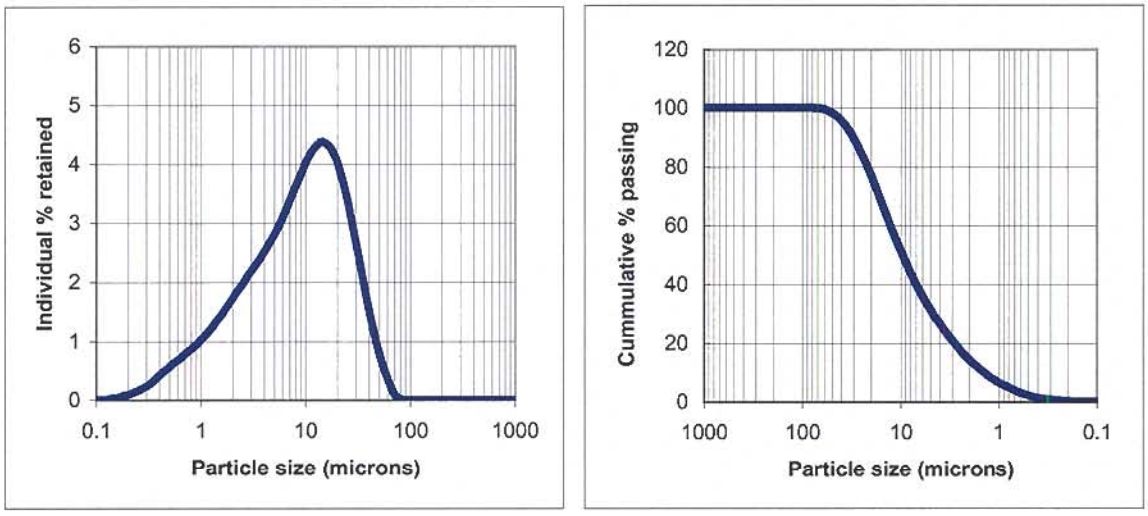


**Figure 3. Particle Size Distribution for Cement DD2**

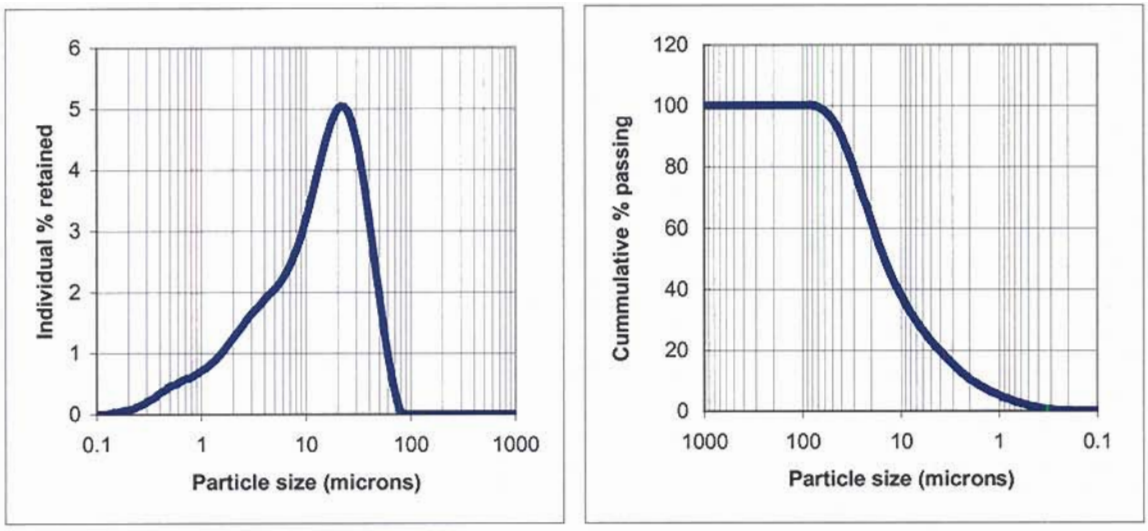


**Figure 4. Particle Size Distribution for Cement EE**

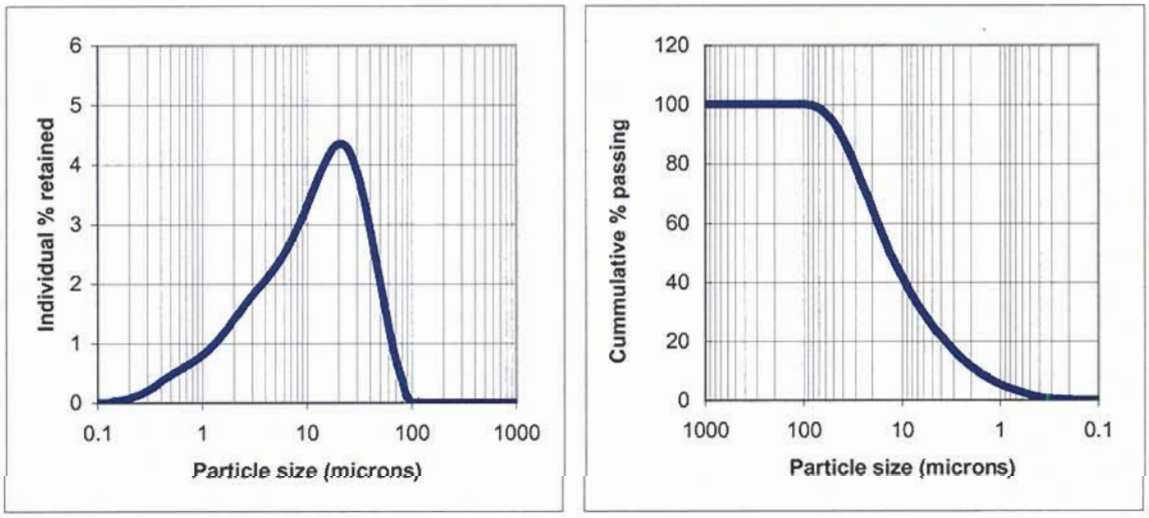


**Figure 5. Particle Size Distribution for Cement PP**

### 3.1.3 Clinker Morphology

In addition to cement compound composition and content, an important parameter that affects cement reactivity and performance is the distribution and characteristics of cement phases. Petrographic examination of cement clinkers was performed to assess the effects of compound morphology on hardened concrete properties. Reflected light microscopy was used for characterizing the clinker. All the clinkers were stained with ammonium nitrate solution and then with potassium hydroxide solution. The first staining colored alite grains dark brown to blue and belite grains light brown. The second staining turned $C_3A$ a bluish gray color, making it more distinctive inside the matrix. The $C_4AF$ was unaffected by either solution and can be observed as the white portion of the matrix. Clinkers' morphology are depicted in Figures 6 through 9.

Clinker CC has the largest alite grains, followed closely by EE and PP. DD-2 clinker has the finest $C_3S$ crystals; this in turn can impact the early strength of DD-2 cement. Alite in cements DD2, EE, and PP was colored light blue and in CC it was stained dark brown to dark blue. This could be attributed to the difference in amount or type of substitutional atoms in the alite of CC clinker compared to the other clinkers.

The belite content for CC cement is obviously less than any other cement. Small inclusions inside the $C_3S$ grains are also noticed as in Figure 6. This observation might impair the latter strength gain of CC cement. In DD2 clinker, belite was very localized, forming streaks and clusters. Belite grains in EE clinker were of smaller size. This may enhance the later strength of EE cement. Belite in PP clinker was well dispersed. Figure 9 illustrates the average size of the belite and alite grains in clinker PP. Belite grains are observed to be of larger size. It is also noted that $C_3A$ grains are abundant. Figure 9 displays the average grain size of $C_3A$ in this clinker, although it does include some unusually large belite particles. Belite crystals in all the clinkers, except for CC, were rounded, with well-defined lamellar structure. The absence of belite in CC implies that strength gain at later ages might be compromised. All the clinkers have a well-defined matrix. PP clinker has the smallest average size of $C_3A$ crystals, which implies that they are highly reactive compared to the other clinkers. $C_3A$ particles in CC, DD2, and EE have similar size and, therefore, similar reactivity.

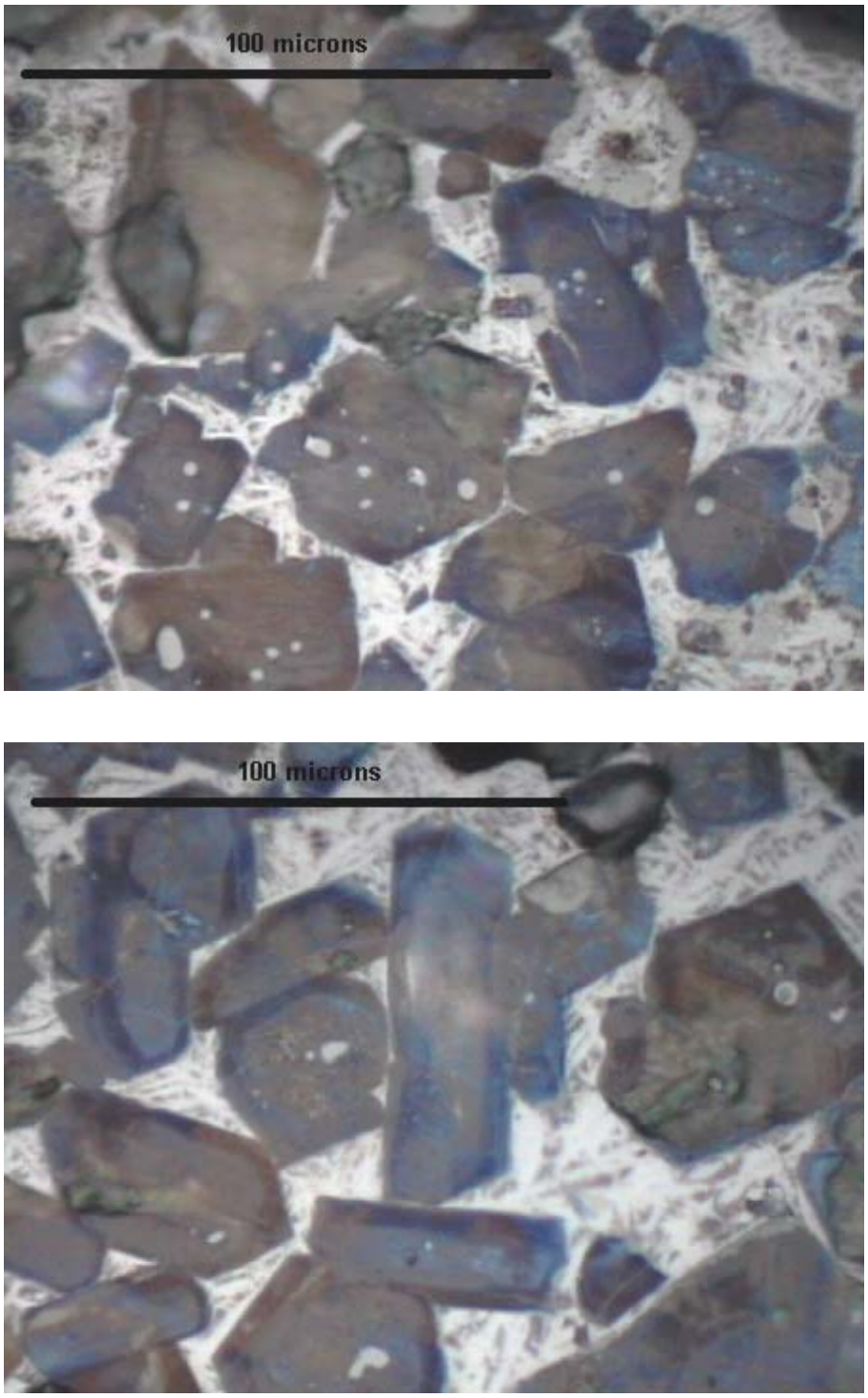


**Figure 6. Reflected Light Microscopy Images of Clinker CC.**

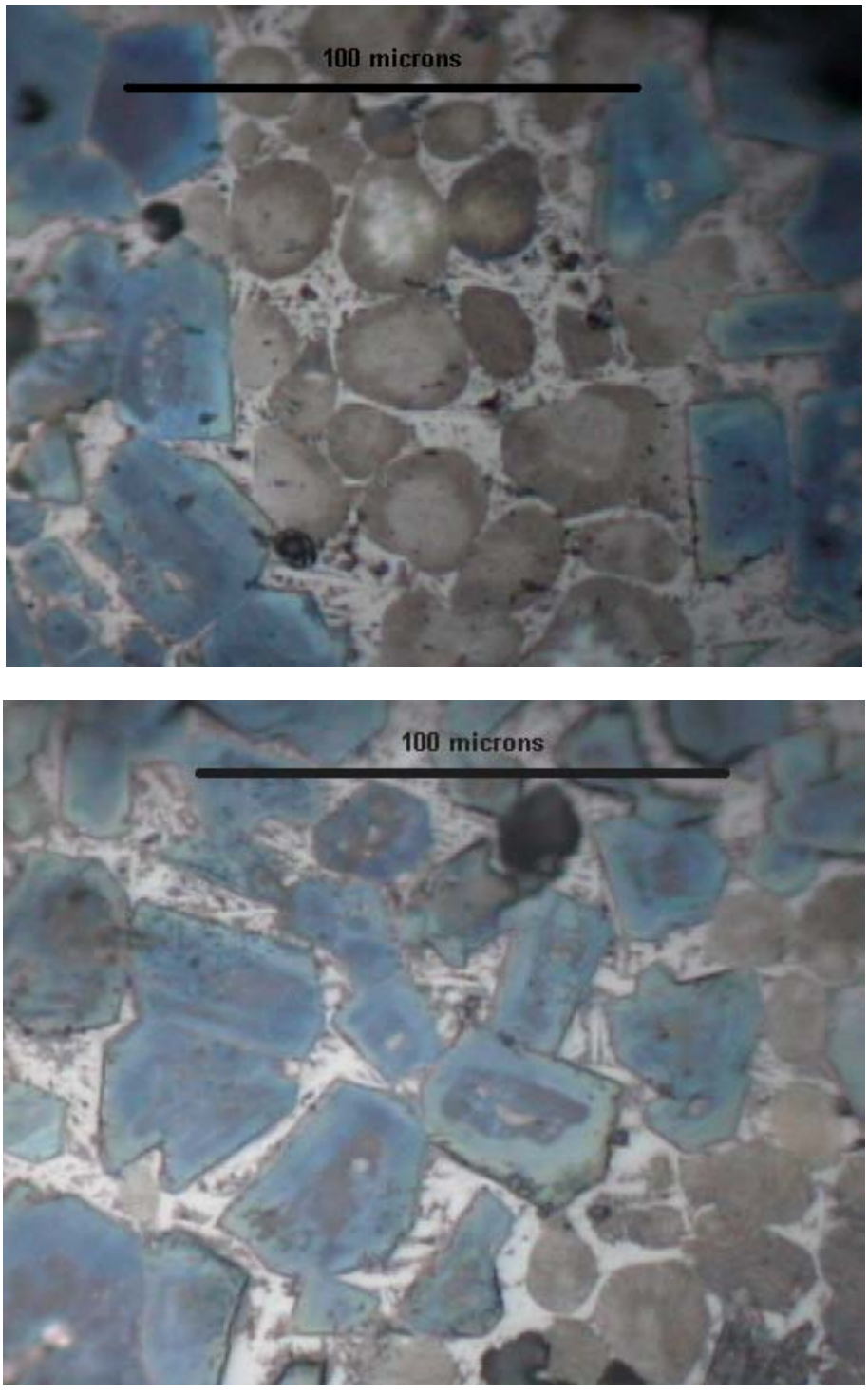


**Figure 7. Morphology of DD-2 clinker**

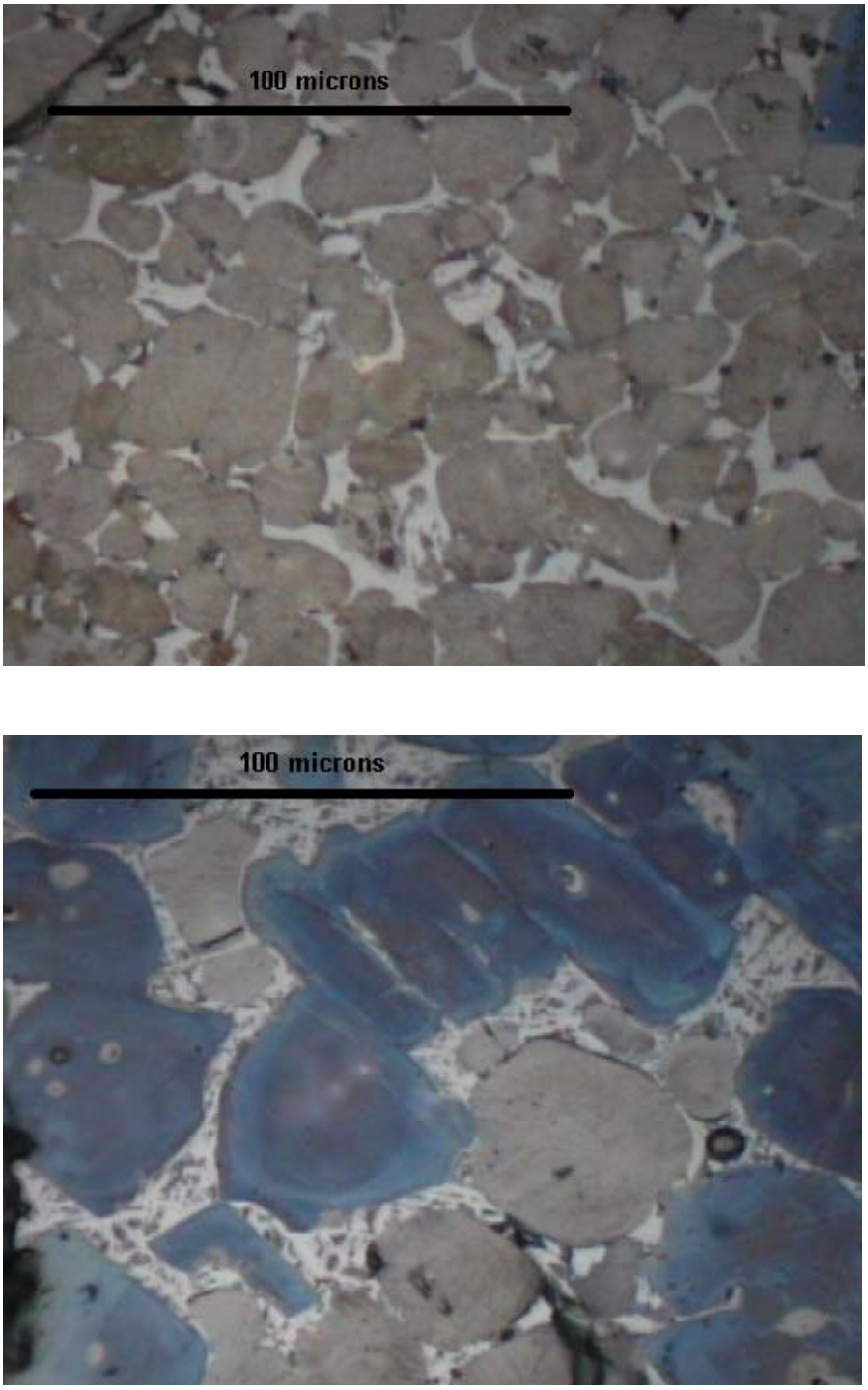


**Figure 8. Morphology of EE Clinker**

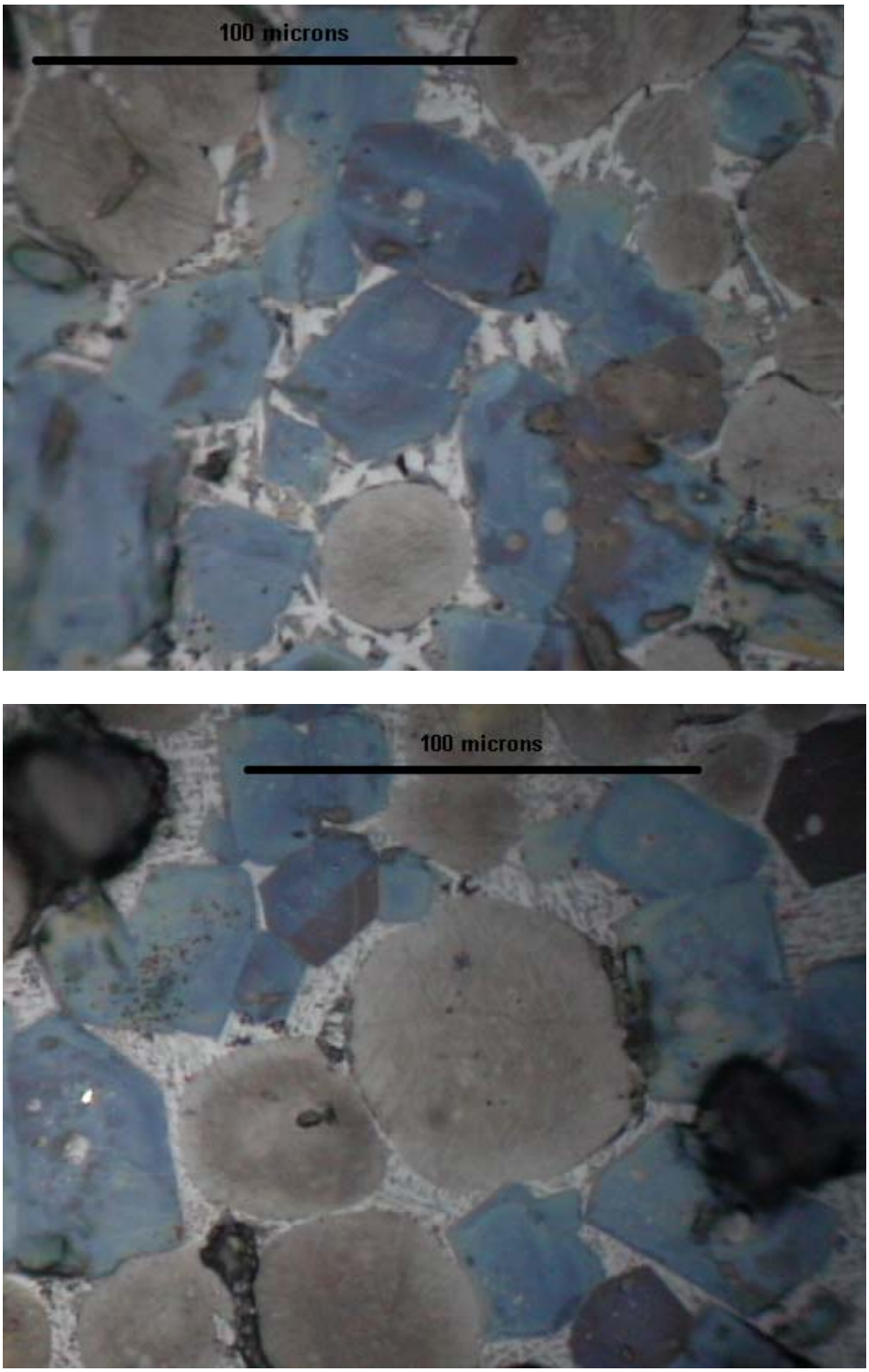


**Figure 9. Morphology of PP Clinker**

### 3.1.4 Oxide Chemical Composition

Oxide chemical composition of the as-received cements was determined using x-ray fluorescence spectroscopy. The results are presented in Table 2. In addition, cements' main compounds compositions were calculated following ASTM C 150-97 (Bogue calculation) as shown in Table 3. The results indicate that cements P and C have a higher $SO_3$ content than cements DD2 and EE. In addition, the alkali content of PP cement is marginally higher than the ASTM set limits. Cements EE and DD2 have similar alkali content while cement CC had the lowest alkali content.

**Table 2. As-Received Cement Oxide Chemical Composition**

| | CC | DD2 | EE | PP |
|---|---|---|---|---|
| **Oxide** | **w/o** | **w/o** | **w/o** | **w/o** |
| **$SiO_2$** | **20.52** | **20.55** | **21.15** | **20.78** |
| **$Al_2O_3$** | **4.92** | **4.4** | **4.78** | **5.47** |
| **$Fe_2O_3$** | **3.7** | **3.61** | **3.76** | **4.15** |
| **CaO** | **64.31** | **64.6** | **64.41** | **63.14** |
| **MgO** | **1.71** | **2.47** | **0.95** | **0.85** |
| **$SO_3$** | **2.81** | **2.54** | **2.58** | **2.88** |
| **$Na_2O$** | **0.01** | **0.03** | **0.18** | **0.26** |
| **$K_2O$** | **0.41** | **0.54** | **0.34** | **0.6** |
| **$TiO_2$** | **0.27** | **0.22** | **0.33** | **0.32** |
| **$P_2O_5$** | **0.03** | **0.05** | **0.07** | **0.18** |
| **$Mn_2O_3$** | **0.04** | **0.05** | **0.03** | **0.03** |
| **SrO** | **0.04** | **0.02** | **0.12** | **0.05** |
| **$Cr_2O_3$** | **<0.01** | **0.02** | **<0.01** | **0.02** |
| **ZnO** | **<0.01** | **0.03** | **0.02** | **0.02** |
| **L.O.I. (950°C)** | **1.08** | **0.99** | **1.15** | **1.3** |
| **Total** | **99.83** | **100.12** | **99.84** | **100.04** |
| **Alkalies as $Na_2O$** | **0.27** | **0.39** | **0.4** | **0.65** |
| **Free CaO** | **0.92** | **2.31** | **1.05** | **0.44** |

**Table 3. Cement Compound Composition [Bogue Calculation]**

| Compound | CC (%) | DD2 (%) | EE (%) | PP (%) |
|---|---|---|---|---|
| $C_3S$ | 60 | 65 | 57 | 48 |
| $C_2S$ | 14 | 10 | 18 | 23 |
| $C_3A$ | 7 | 6 | 6 | 7 |
| $C_4AF$ | 11 | 11 | 11 | 13 |
| $C_3S/C_2S$ | 4.3 | 6.5 | 3.2 | 2.1 |

From Table 3 it can be seen that all cements studied here have similar tricalcium aluminate content (6-7 w/o) and a wide span of tricalcium silicate content (48 to 65 w/o). Tetracalcium aluminoferrite was also similar in all cements (11-13%). Based on the oxide chemical analysis and Bogue calculations, all cements studied here are classified as Type I ASTM cements.

### 3.1.5 Mineralogical Composition

It is well established that the cement compound content as determined from Bogue calculations, are essentially an approximation. Therefore, mineralogical phase quantification for as-received cements was done using x-ray diffraction. Phase quantification was determined by two methods; namely, internal standard method and Rietveld analysis.

The $C_3S$ calibration curve was built using a laboratory prepared sample of monoclinic alite. Monoclinic alite can has four polymorphs: M1, M2, M3 sublattice, and M3 superlattice [4]. Visual identification method described by Courtial [5] was used to determine which monoclinic polymorphs were present in the sample. After observing the five angular windows recommended by Courtial, it was concluded that the laboratory prepared alite consisted mostly of the M3 polymorph. However, the shape of the peak in the 51-53° 2θ window suggests that the sample has possibly small traces of M1 polymorph. However, for the purpose of this study, the sample was assumed to be made entirely of M3 polymorph. This is due to the limitations of the available programs on Rietveld analysis where insertion of two phases of the same chemical formula and crystal system with only minor differences in their crystal structure results in failure of Rietveld refinement [4].

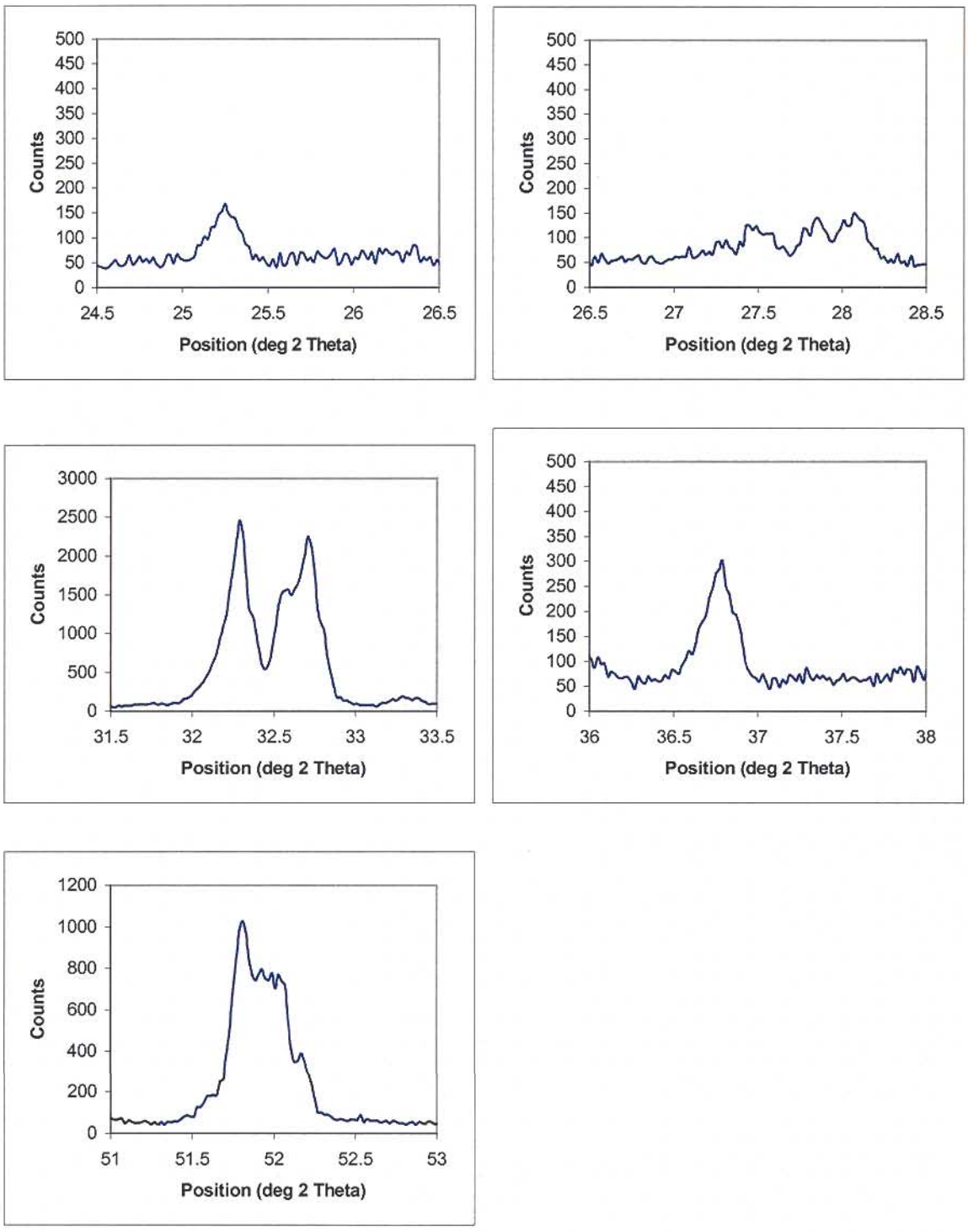


**Figure 10. Five Windows Used for the Monoclinic Alite Polymorph Identification**

The advantage of using the internal standard method is that it allows for one phase to be quantified without determining the amounts of the other phases present in the sample [3]. It is ideal to use a material for building the calibration curves with the exact chemical composition and crystal structure, as it is present in the samples to be analyzed. However, this is often impossible when dealing with cement samples due to numerous possible substitutional ions and crystal system polymorphs. Preferred orientation as well as peak overlap is also a concern when using the internal standard method [3]. Care was taken to select peaks free from preferred orientation and with minimal amount of overlap from other phases. As the focus of this study was the tricalcium silicate content, quantification using the internal standard method was limited to tricalcium silicate content. Results of phase quantification using internal standard x-ray diffraction techniques are presented in Table-4.

**Table 4. As-Received Cement Tricalcium Silicate Content (XRD Internal Standard Method)**

| | Cement (%) | | | |
|---|---|---|---|---|
| **Compound** | **CC** | **DD2** | **EE** | **PP** |
| **$C_3S$** | **70** | **63** | **58** | **55** |

Comparing the results of Table 4 to Table 3 indicates that there is a significant difference in the tricalcium silicate phase content as determined by both methods. This is an expected finding consistent with the published literature. Phase quantification based on Bogue analysis is typically an approximation.

Crystal structures used in the Rietveld refinement analysis for monoclinic alite are: M3 superlattice structure [6] and M3 sublattice structure [7]. After several initial refinements, Nishi superstructure was used for quantification because it provided a better fit for all the cements. This structure seemed to be more flexible, which could be attributed to a much higher number of atomic positions (226 in the Nishi structure compared to 21 in the Mumme structure). Figures 10-15 show the final Rietveld refinement profiles for all the cements. Figure 10 presents two of several angular windows that are commonly used to identify the structure of $C_3S$ [2, 5]. This figure

clearly illustrates the differences between the alite structures in the cements. Figures 11 through 15 show the collected XRD pattern (red) and calculated pattern (blue). Vertical lines correspond to the peak positions of different phases, one color per phase. Also shown is a difference plot between the collected and the calculated patterns.

Results of the refinement are presented in Table 5 and 6. In general, phase quantification from the internal standard method and Rietveld refinement is in better agreement than if compared with the Bogue calculations. From both XRD methods, tricalcium silicate seems to be lowest in PP cement while highest in CC cement. Though the trends of tricalcium silicate from both XRD methods are in agreement, both methods are in disagreement with the Bogue analysis. CC cement has the highest tricalcium silicate content as determined by XRD while DD2 cement has the highest content as determined through the Bogue calculations.

Rietveld Analysis also indicates that PP cement has the highest C3A content while CC, DD2 and EE are essentially similar in their $C_3A$ content. Due to the low $C_3A$ content in cements, extractions are indicated. Results of the analysis performed on the extracted and ignited cements are presented in Table 6. They confirm the $C_3A$ values listed in Table 5. In the case of $C_3A$, there are only minor variations between the internal standard method and Rietveld refinement results. The variance in the $C_3S$ content is not significant either: between 2 and 4 %. This variance could be attributed to the fact that even though the $C_3S$ is present in the monoclinic form in all the cements, the combination of the monoclinic polymorphs is different for each cement. .

**Table 5. Rietveld Refinement Results for the Ground As-Received Cements**

| | Cement | | | |
|---|---|---|---|---|
| **Compound** | **CC** | **DD2** | **EE** | **PP** |
| **$C_3S$** | **67** | **61** | **54** | **53** |
| **β-$C_2S$** | **15** | **19** | **25** | **23** |
| **Cubic $C_3A$** | **2** | **3** | **4** | **9** |
| **$C_4AF$** | **14** | **12** | **13** | **11** |
| **Gypsum ($Ca_2SO_4.2H_2O$)** | **--** | **--** | **2.0** | **0.9** |
| **Bassanite ($Ca_2SO_4.0.5H_2O$)** | **1.5** | **1.6** | **1.6** | **0.7** |
| **Anhydrite ($Ca_2SO_4$)** | **1.3** | **--** | **--** | **--** |
| **Calcite ($CaCO_3$)** | **--** | **--** | **--** | **--** |
| **Magnesite ($MgCO_3$)** | **--** | **--** | **--** | **1.8** |
| **Periclase (MgO)** | **--** | **1.8** | **--** | **--** |
| **Dolomite ($CaMg(CO_3)_2$)** | **--** | **0.9** | **--** | **1.2** |
| **Portlandite ($Ca(OH)_2$)** | **--** | **1.2** | **--** | **--** |

**Table 6. Rietveld Refinement Results from SAM Extractions on Cements**

| | Cement | | | |
|---|---|---|---|---|
| **Compound** | **CC** | **DD2** | **EE** | **PP** |
| **Cubic $C_3A$** | **3** | **4** | **4** | **8** |
| **Periclase (MgO)** | **0.1** | **1.9** | **--** | **--** |
| **Anhydrite ($Ca_2SO_4$)** | **3.0** | **2.6** | **3.5** | **3.7** |

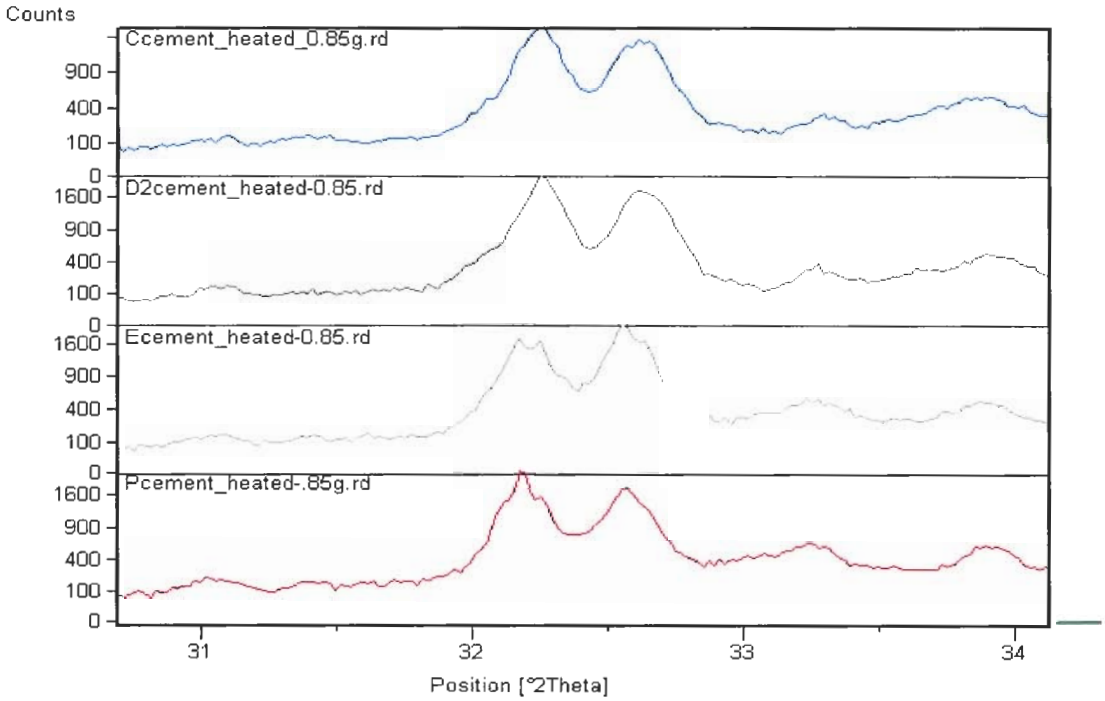


**Figure 10.1 XRD Pattern for As-Received Cements; 2θ = 30.6° – 34.2°**

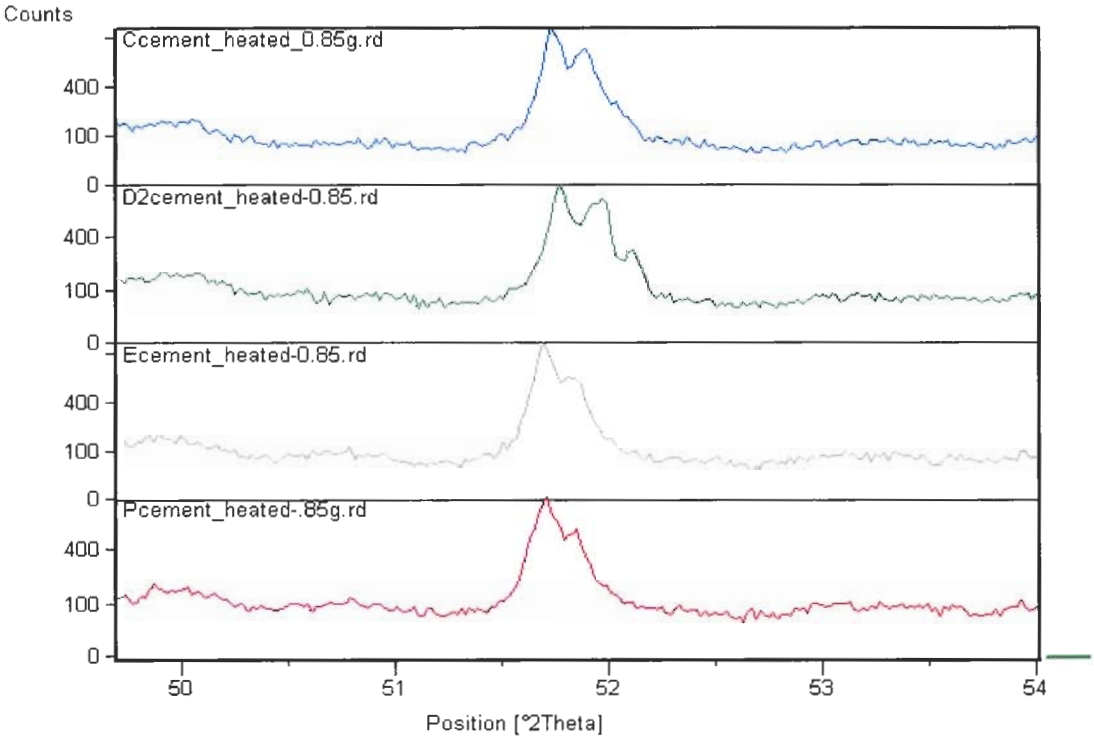


**Figure 11 XRD Pattern for As-Received Cements; 2θ = 49.5° – 54°**

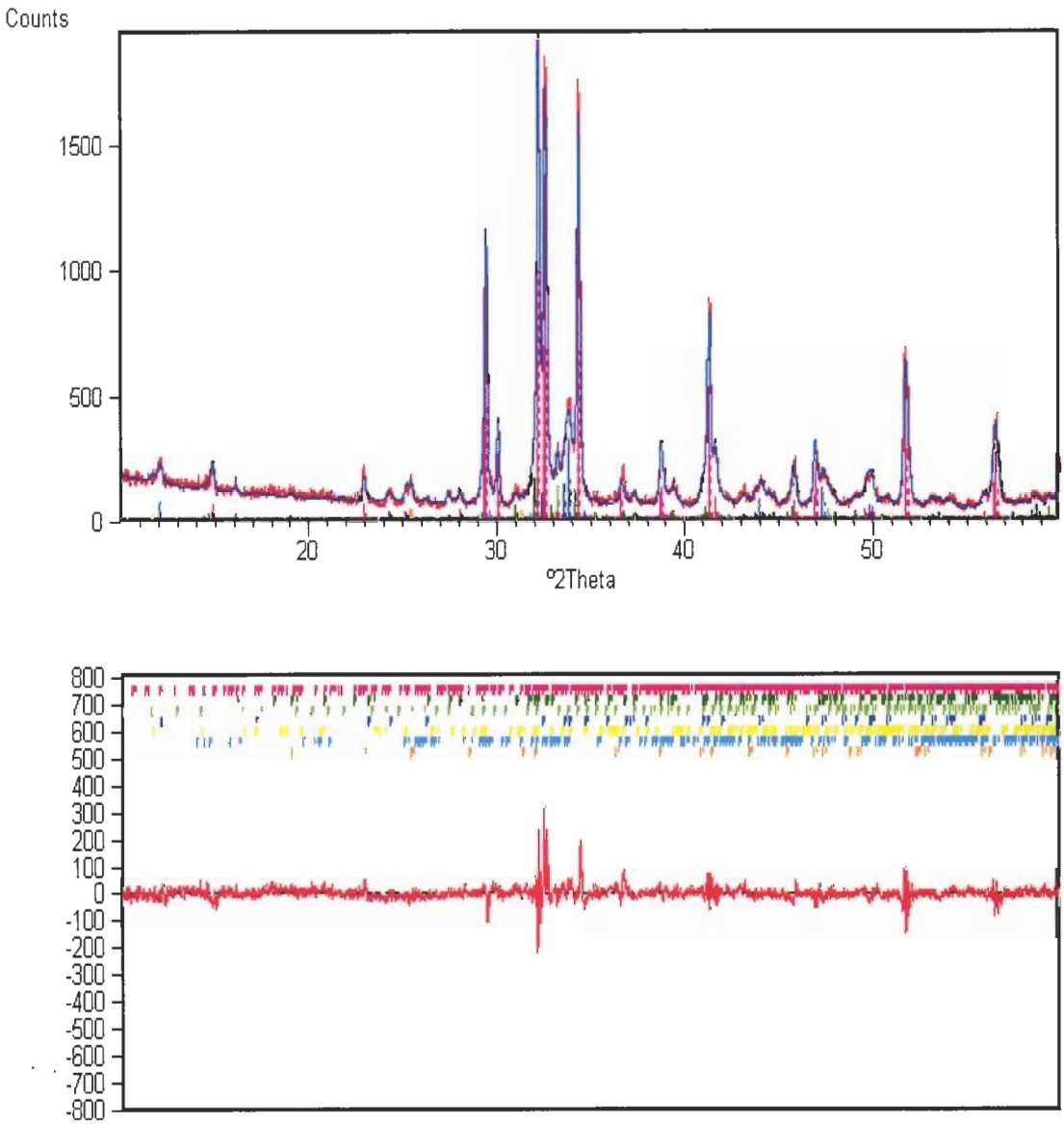


**Figure 12. Rietveld Refinement for As-Received Cement CC**

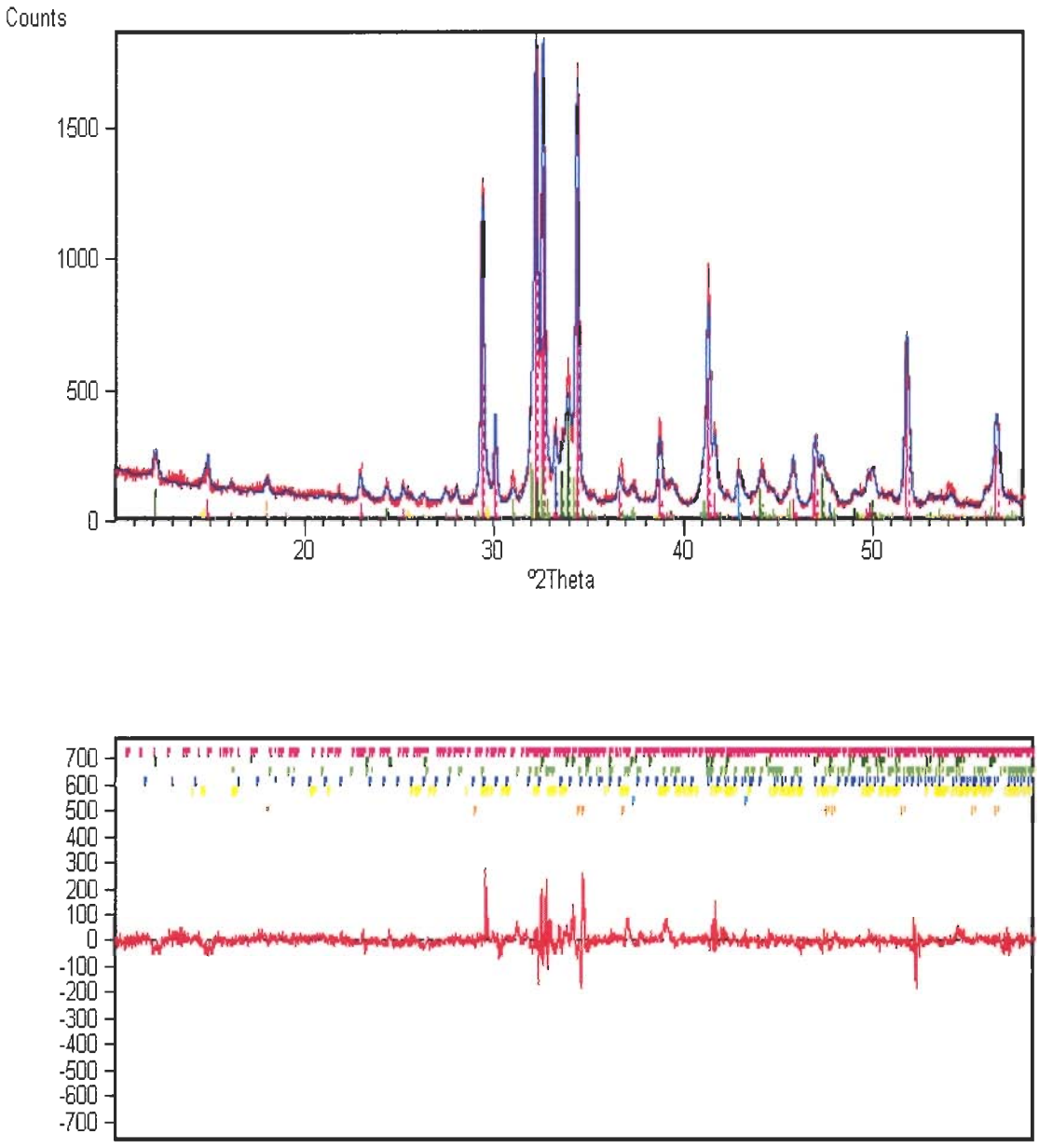


**Figure 13. Rietveld Refinement for As-Received Cement DD2**

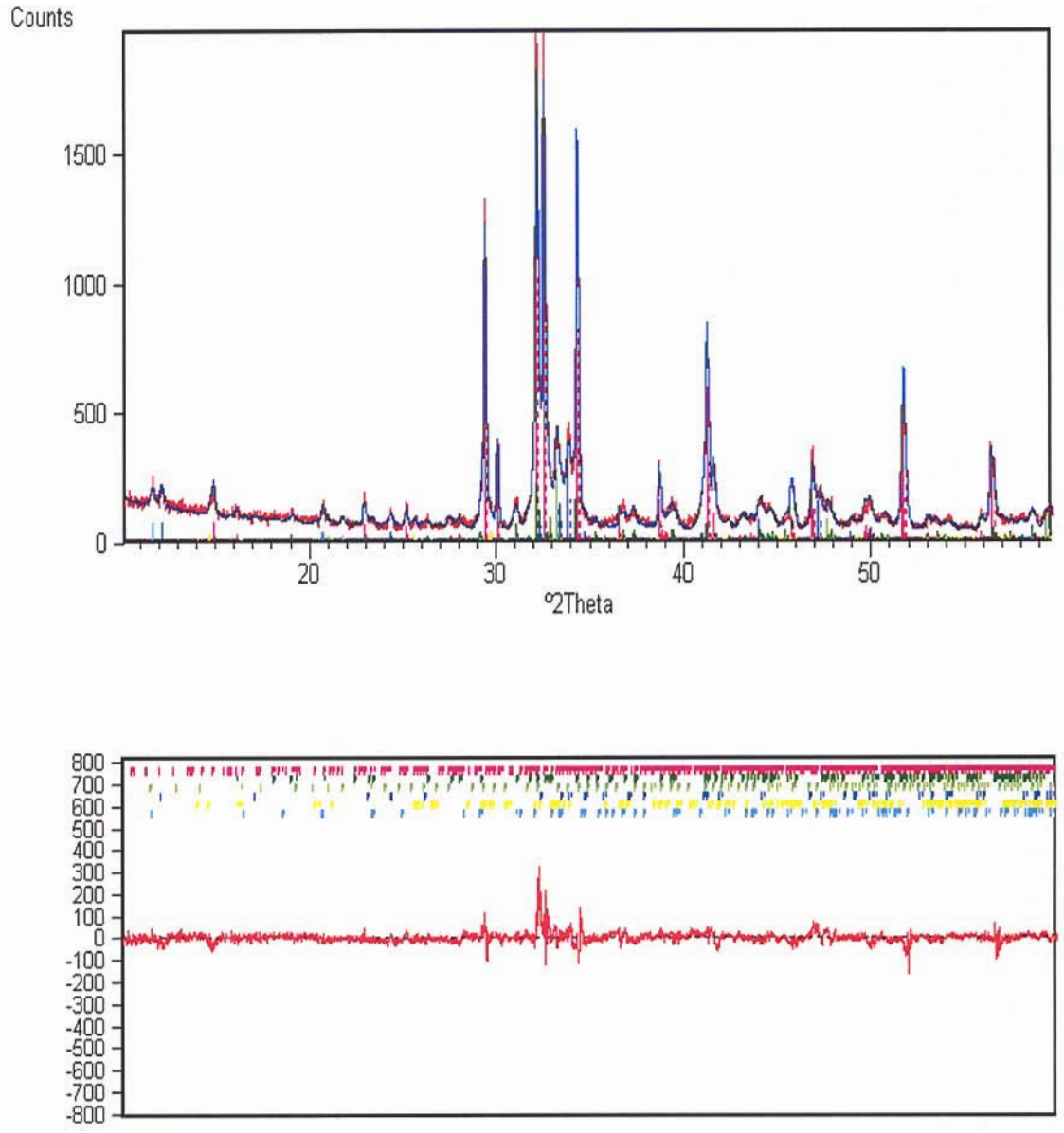


**Figure 14. Rietveld Refinement for As-Received Cement EE**

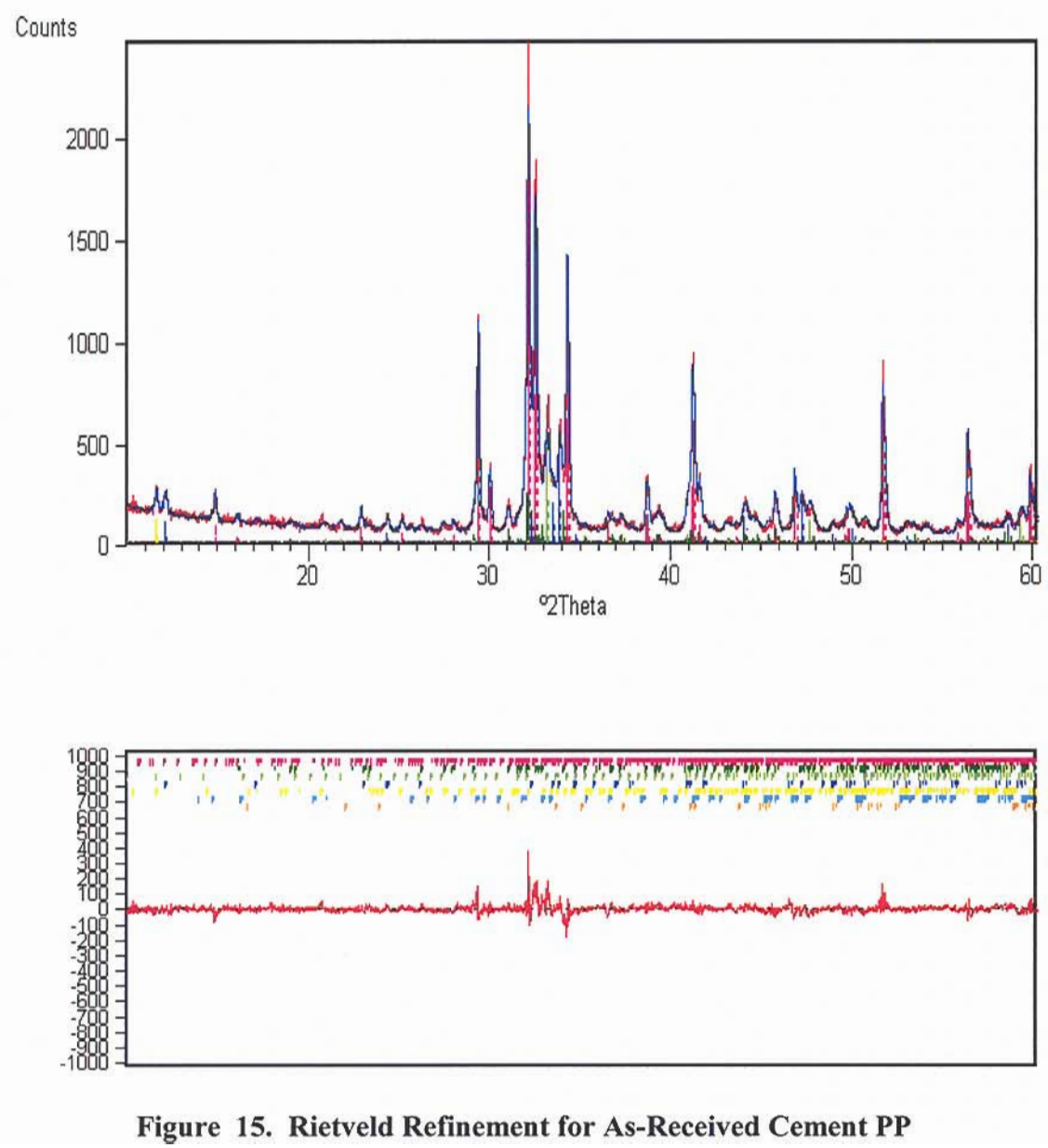


**Figure 15. Rietveld Refinement for As-Received Cement PP**

In conclusion, analysis of the as-received cements indicates that there is a significant difference in the tricalcium silicate content, which is what is required to address the purpose of this investigation. In addition, the analyses performed on the as-received cements indicate that though as-received cements have similar Blaine fineness, they have differences in their particle size distribution.

## 3.2 Durability

### 3.2.1 Mortar Linear Expansion in $Na_2SO_4$ Solution

Length changes experienced by mortar bars exposed to sodium sulfate solution (5%) are presented in Figure 16. For each of the as-received cements, six mortar bars were prepared in accordance with ASTM C 1012. Overall, CC bars had the highest expansion of 1% at 330 days. Among cements with similar tricalcium aluminate content EE cement experienced significantly less expansion than cement CC by approximately an order of magnitude. Cement DD2 experienced similar expansion behavior to cement CC. Though cements CC, DD2 and EE have similar tricalcium aluminate content, which is about half that present in cement PP, the expansion trends seems to depend on tricalcium silicate content of the cement.

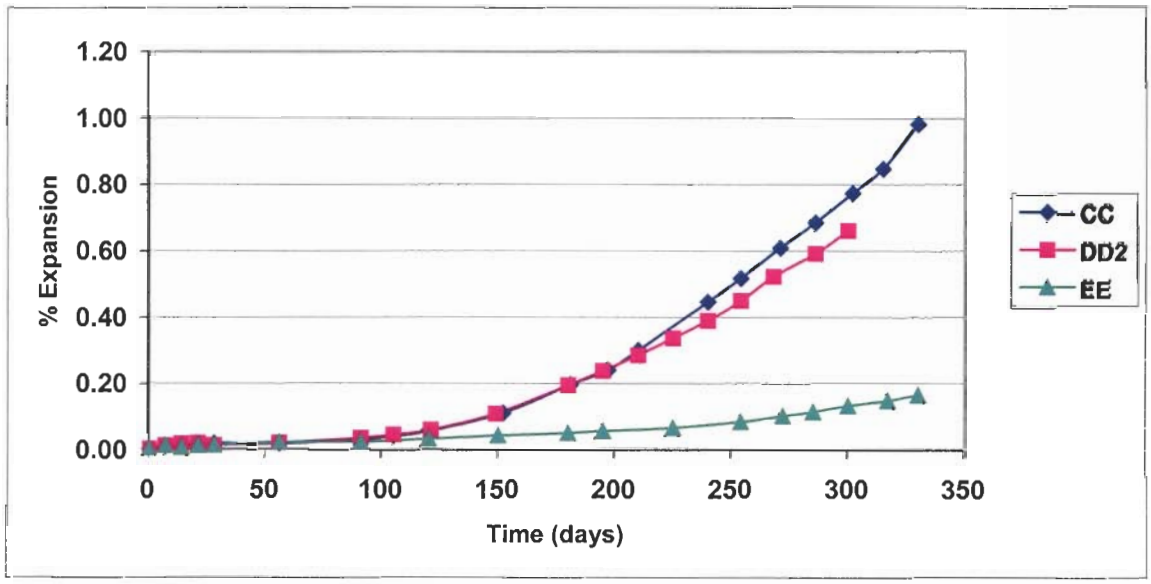


**Figure 16. Expansion of Mortar Bars Prepared with As-Received Cements**

In order to verify the observed trends, as-received cements PP and EE were doped with lab prepared tricalcium silicate. The tricalcium silicate content of those two cements was increased by 21 % for PP cement and by 12% for EE cement. Table - 7 shows the tricalcium silicate and aluminate content prior to and following doping.

**Table 7. Tricalcium Silicate and Aluminate Content Prior and After Doping [Bogue]**

| Cement | % C3S (As-received) | % C3S (Doped) | % C3A (As-received) | % C3A (Doped) |
|---|---|---|---|---|
| PP | 48 | 69 | 7 | 7 |
| EE | 57 | 69 | 6 | 6 |

Figures 17 and 18 show the expansion of the mortar bars that were doped with alite. At 120 days, PP-D bars have expanded dramatically (1.9%), approximately an orders of magnitude higher, than the as-received PP. Similar observations are reported for EE-D. At an age of 150 days, the expansion for the latter was 3-folds higher than its as-received counterpart. The differences in degree of expansion are attributed to differences in tricalcium aluminate content of cements.

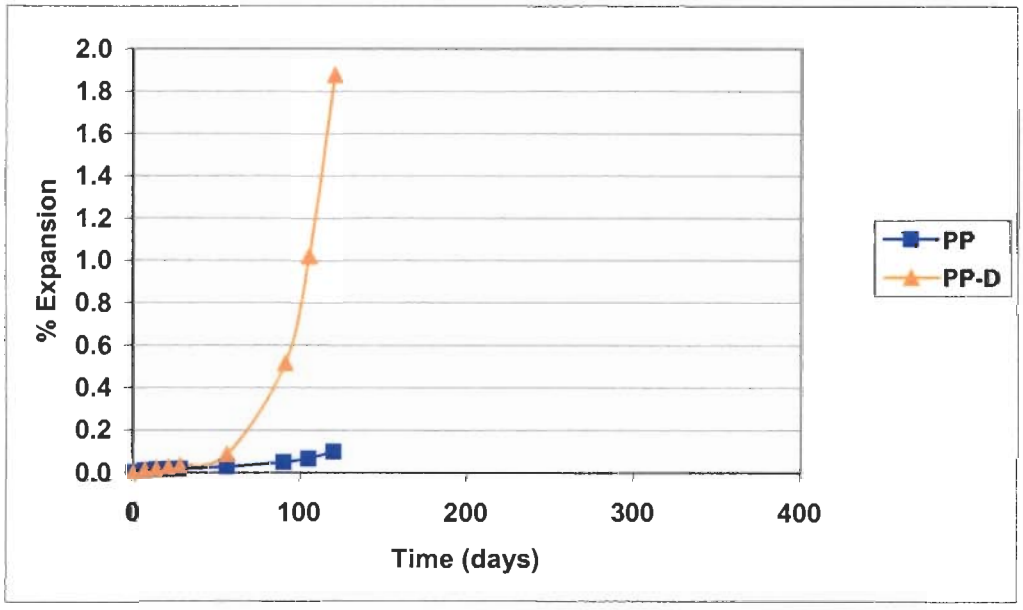


**Figure 17. Expansion of Mortar Bars Doped with 21%$C_3S$**

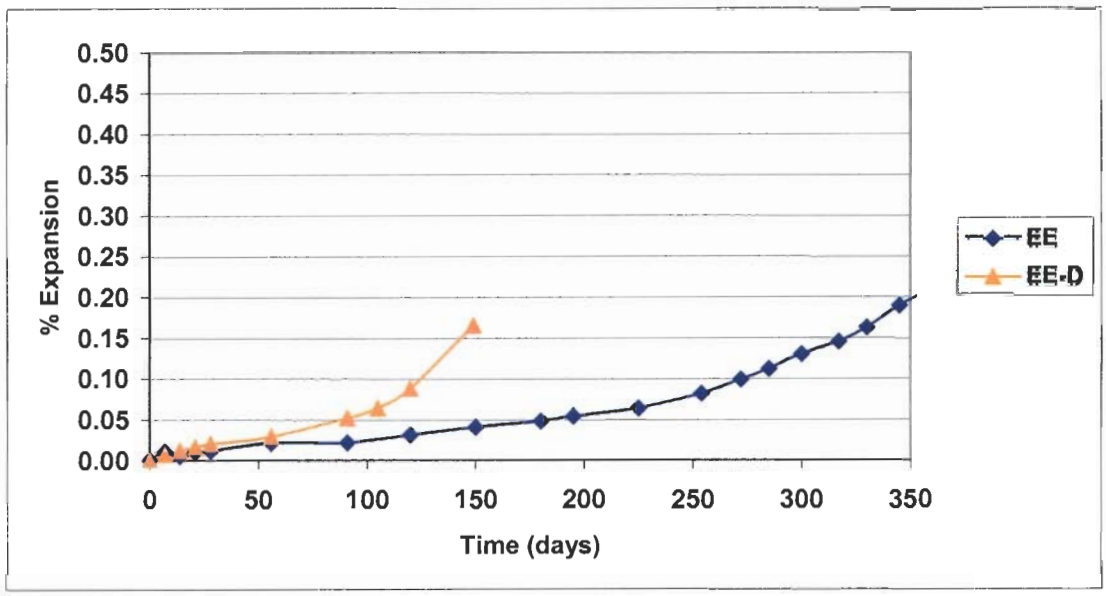


**Figure 18. Expansion of Mortar Bars for EE Cement Doped with 12%$C_3S$**

In conclusion, the results indicate that increasing tricalcium silicate content is of significance to sulfate durability. The effect is more pronounced in cements with higher tricalcium aluminate content.

### 3.2.2 Mortar Cube Strength

Compressive strength of mortar cubes stored in saturated lime solution is displayed in Figure 19. The strength of mortar cubes in lime shows that EE cement has the highest ultimate strength. This is attributed to its high dicalcium silicate content, as depicted in Table 6. PP cement has a high dicalcium silicate content similar to EE; however, its ultimate strength is lower than EE cement. It appears, though, to be still gaining strength. However, for the high tricalcium silicate cements, the strength gain beyond 120 days seems to be minimal as compared to the low tricalcium silicate/high dicalcium silicate cements PP and EE.

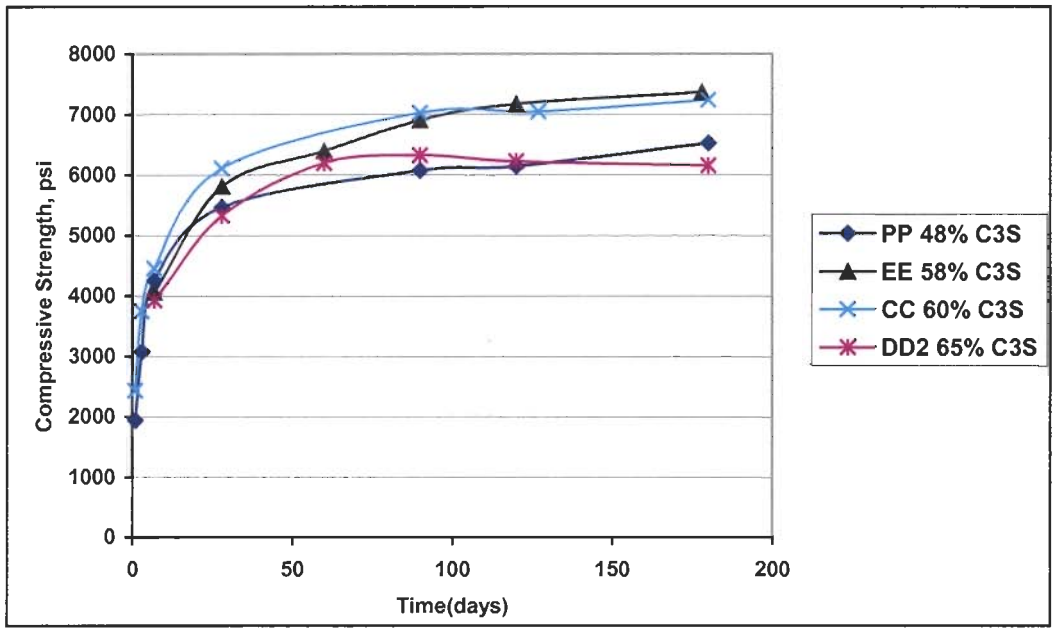


**Figure 19. Compressive Strength of Mortar in Lime Solution**

The effect of sulfate exposure on mortar cube strength is depicted in Figures 20 through 25. It appears that for cements low in tricalcium silicate content, strength of mortar cubes exposed to sulfate solution was higher than those exposed to lime solution up to 120 days of exposure. However, a drop in strength was observed at 180 days of exposure to sulfate solution. For the high tricalcium silicate cement mortars, beyond 28 days, strength of mortar exposed to sulfate solution was lower than that for mortars exposed to lime. This is more apparent in the case of CC mortar cubes where sulfate exposure results in strength drop of 1150 psi at 180 days.

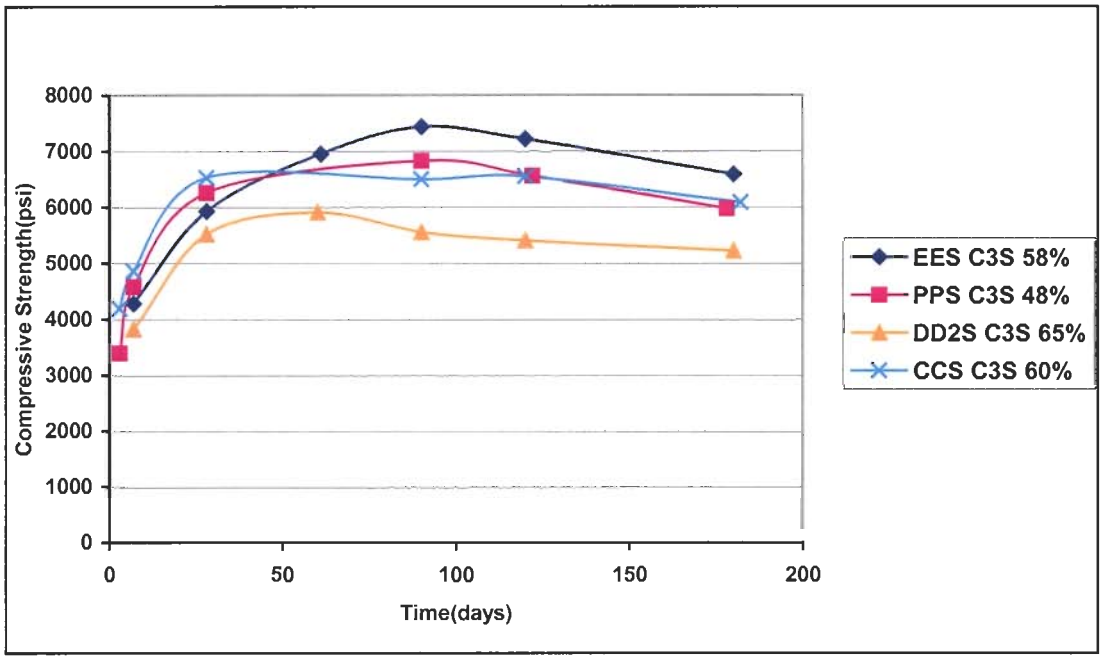


**Figure 20. Mortar cube strength as a function of exposure time to sodium sulfate solution**

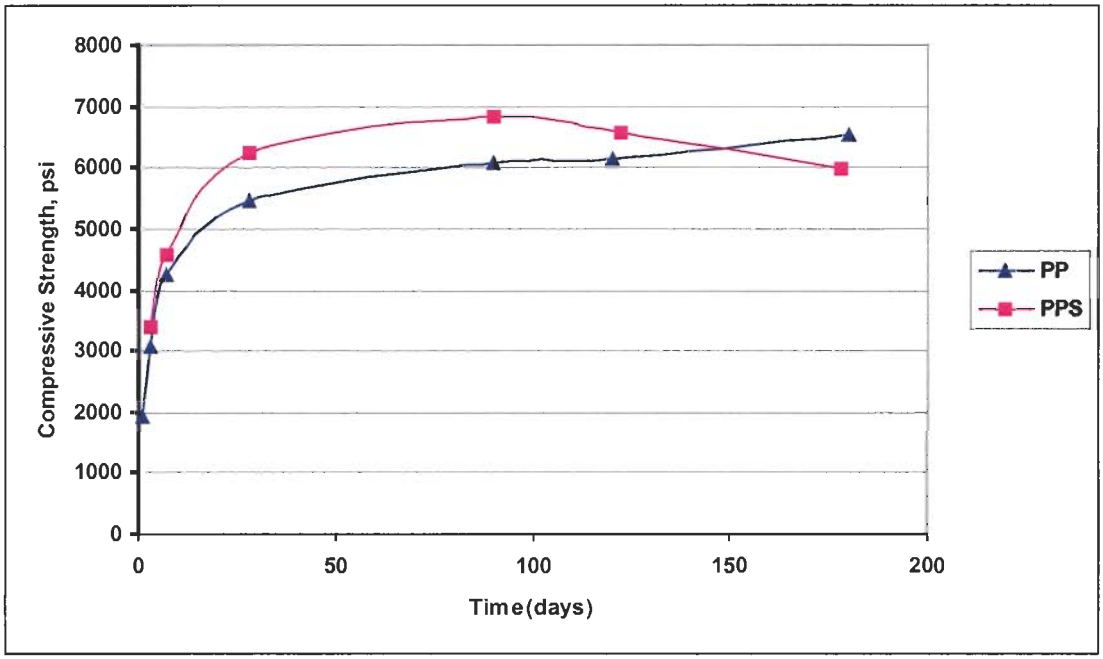


**Figure 21. Compressive Strength of Mortar Cubes in Lime and Sulfate Solution**

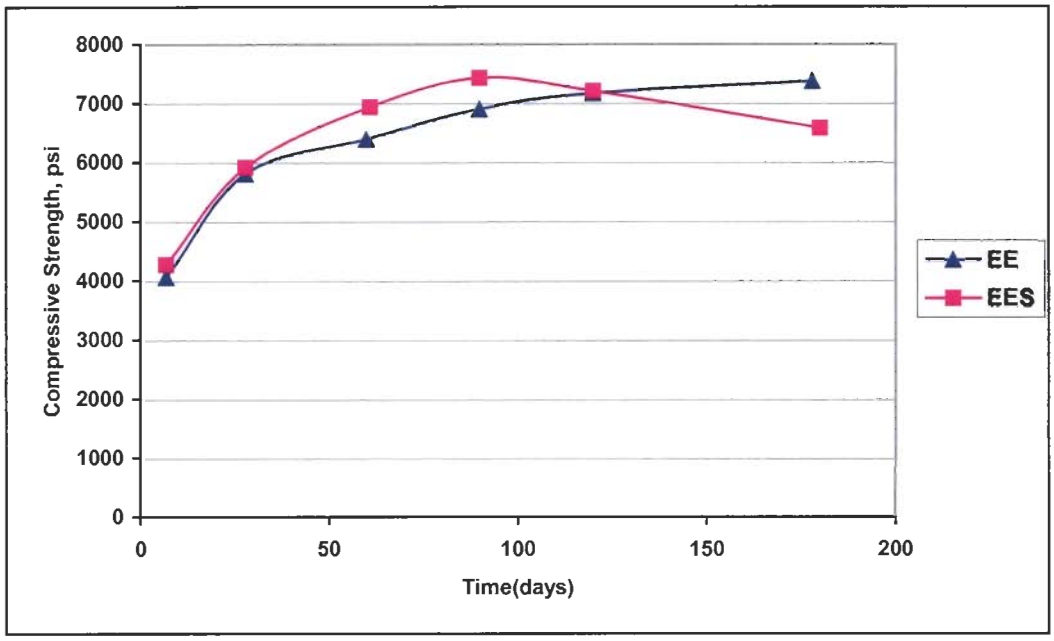


**Figure 22. Compressive Strength of Mortar in Lime and Sulfate Solutions**

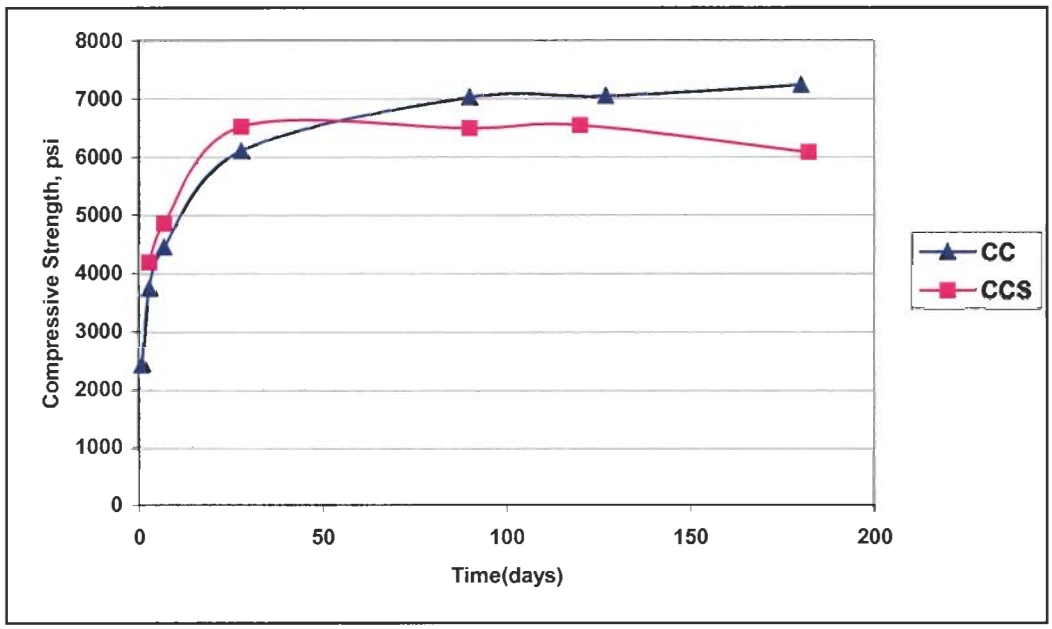


**Figure 23. Compressive Strength of Mortar Cubes in Lime and Sulfate Solutions**

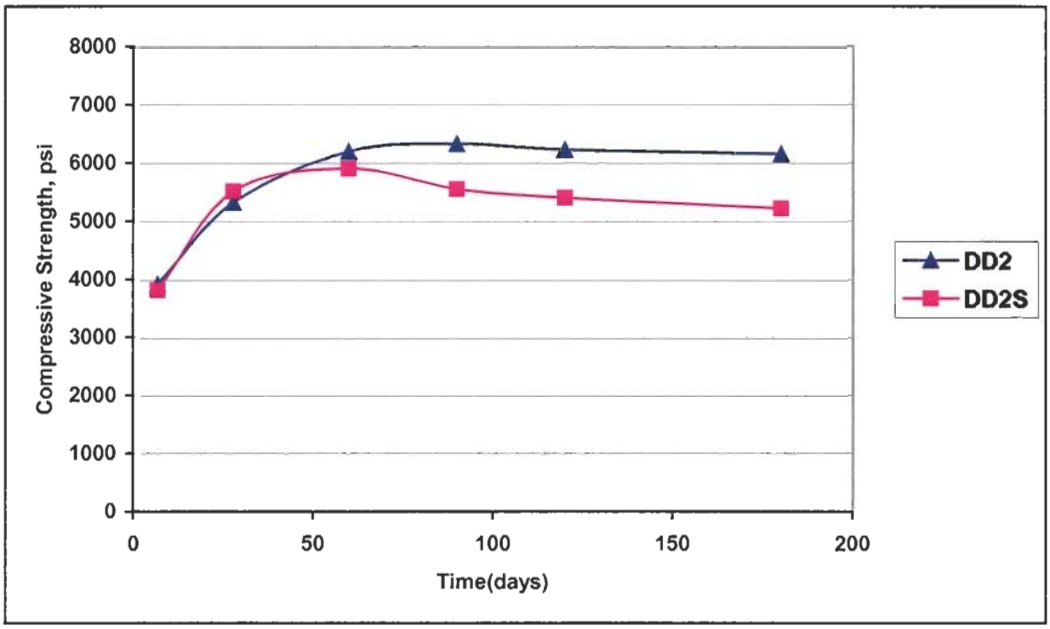


**Figure 24. Compressive Strength of Mortar Cubes in Lime and Sulfate Solutions**

Further verification of the observed trends can be seen from Figure 25, where PP cement was doped by lab prepared tricalcium silicate. Increasing the tricalcium silicate content of this comparatively lower tricalcium silicate cement by 21% $C_3S$ initiated an early drop in the compressive strength for cubes exposed to sulfate solution. Doping PP cement with laboratory prepared alite is of significance to the compressive strength of mortar cubes. The 28-day compressive strength of both sets of cubes was approximately constant. However, by 120 days, the compressive strength of PP-D cement doped with $C_3S$ has dropped by 1000 psi from its 28-day strength value. In addition, at 120 days, comparing the as-received with the doped cement indicates strength drop of more than 1500 psi.

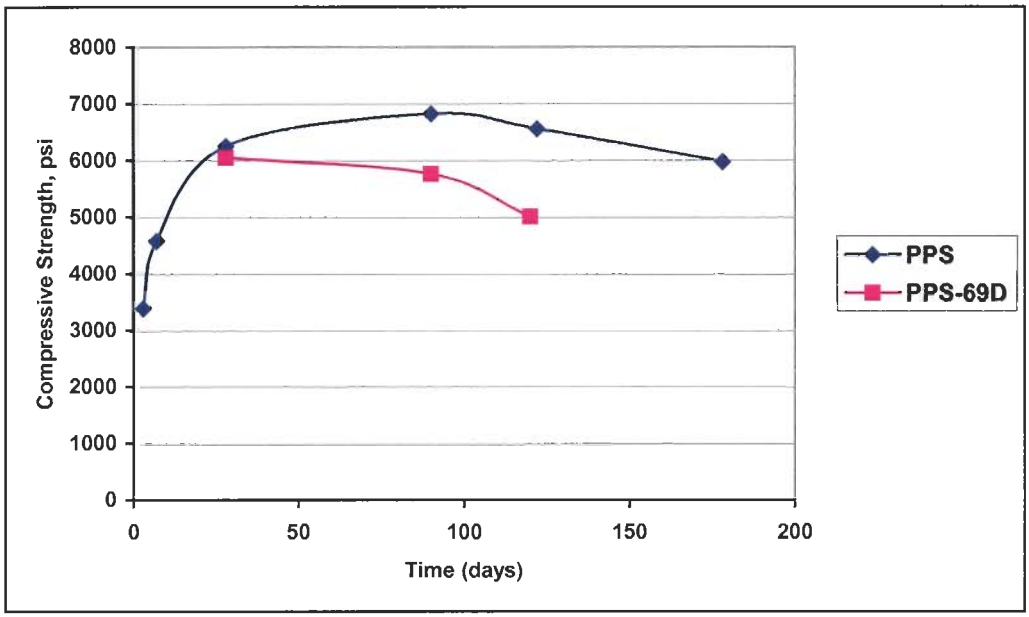


**Figure 25. Effect of Tricalcium Silicate on Mortar Strength in Sodium Sulfate Solution**

In conclusion, the effect of increasing tricalcium silicate in Portland cements on its sulfate durability is clear. In general there seems to be a correlation between tricalcium silicates and strength drop associated with exposure to a sulfate environment. The extent of strength drop appears to increase with tricalcium aluminate content.

### 3.2.5 Concrete Properties

Class II concrete mix was adopted for this part of the investigation. Water to cement ratio was maintained constant and the slump was allowed to vary. For each cement, 70 cylinders were prepared in order to assess the compressive strength, RCP and open-circuit potential (OCP) measurements. It is to be noticed that aggregates used for this part of the study were graded prior to batching. This procedure is adopted in order to maintain uniformity of the aggregates grading curve. Results of variation in strength as a function of exposure time to sodium sulfate solution are depicted in Figure 26.

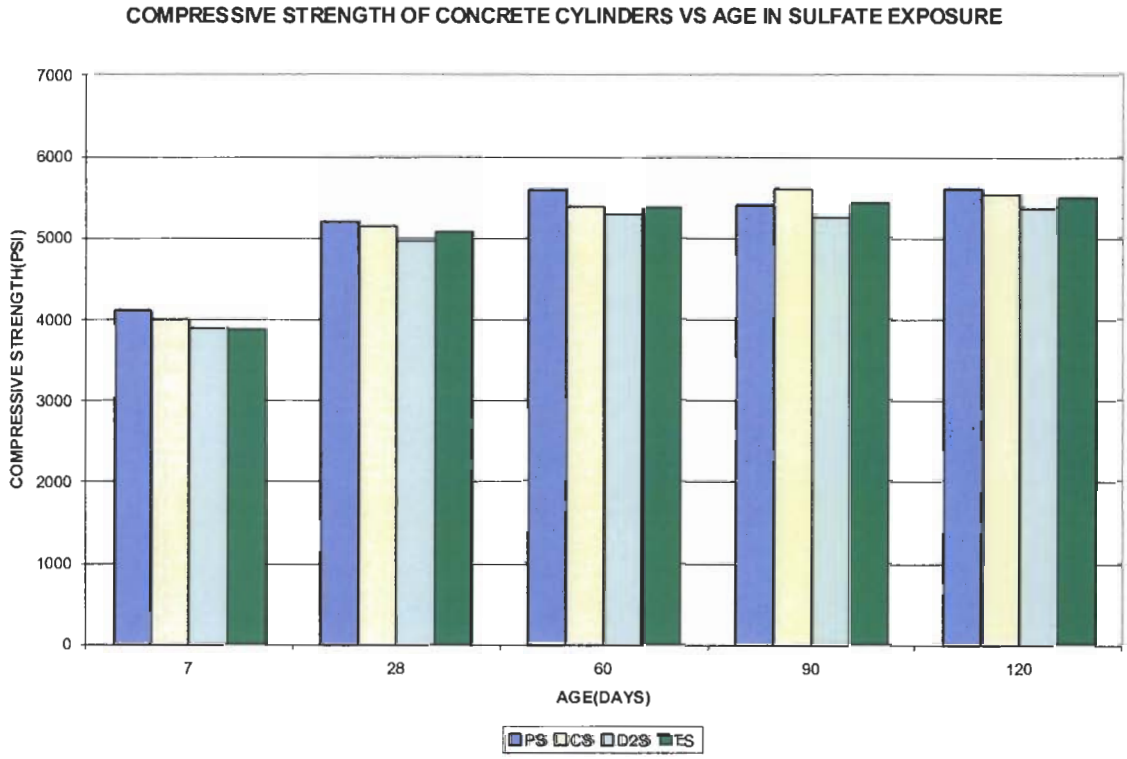


**Figure 26. Variation of Concrete Compressive strength as a function of exposure time to sodium sulfate solution**

The results depicted in Figure 26 indicate that at an age of 120 days CC concrete is the only one that shows a decline in its compressive strength. It is to be noted that CC cement has the highest tricalcium silicate content among the cements studied here. This finding is in agreement with the mortar cube strength results.

Rapid chloride permeability results for concrete cylinders exposed to a 5% sodium sulfate solution are presented in Table 8. RCP measurements were conducted by the Gainesville Materials Research Office, of the Florida Department of Transportation.

**Table 8. RCP Test Results for Specimens cured in 5w/o sodium sulfate solution for Class II Concrete Mix (minimum strength @ 28 days=4,500 psi)**

| Cement | Charge at 28 days (C) | Charge @ 60 days ( C ) | Chage @ 120 days ( C ) |
|---|---|---|---|
| PP | 5968 | 5933 | 3876 |
| EE | 6091 | 5265 | 3858 |
| DD2 | 6196 | 6012 | 4702 |
| CC | 7893 | 6557 | 6434 |

.

As the concrete cylinders were cured in sodium sulfate solution, to the specified testing age, it is anticipated, when analyzing the data, that sulfate resistance of each cement will have an impact on the results of this test. The strength and expansion data, presented previously, indicates the significance of tricalcium silicate on sulfate durability. Though the nature of the deterioration mechanism(s) is not yet addressed, it remains clear that deterioration is effectively rendering the microstructure of the paste more prone to the ingression of aggressive ions. Considering the results of RCP measurements, it appears that there is a correlation between tricalcium silicate content of the cement and chloride permeability expressed as charge passed. Low tricalcium silicate cements (PP, EE) had values less than 4,000 coulombs at 120 days as opposed to high tricalcium silicate cements. Cements CC and DD2 showed values in the high range, 6434 and 4702 coulombs respectively.

Plotting the charge passed at 120 days as a function of tricalcium silicate content of the cements reveals a linear relationship with high r-squared value (Figure 27). In conclusion, RCP results indicate that trcialcium silicate content affects chlorides ingress in concrete.

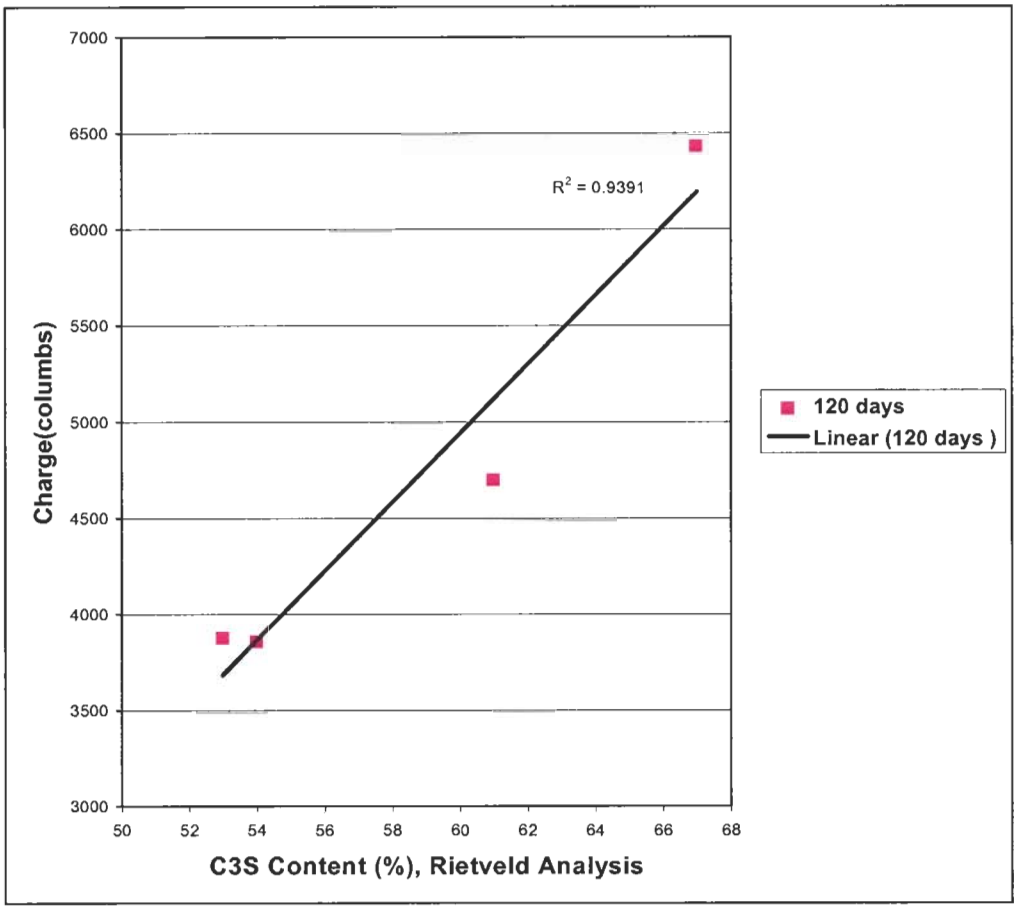


**Figure 27. RCP versus $C_3S$ Content of Cements**

Open-circuit potential measurements for concrete cylinders are presented in Figures 28 through 31. A common feature for all cements is that there is a drop in potential experienced by one of the three specimens. This drop is indicative of active behavior. Longer exposure times are required for assessing the effects of high tricalium silicate on corrosion behavior.

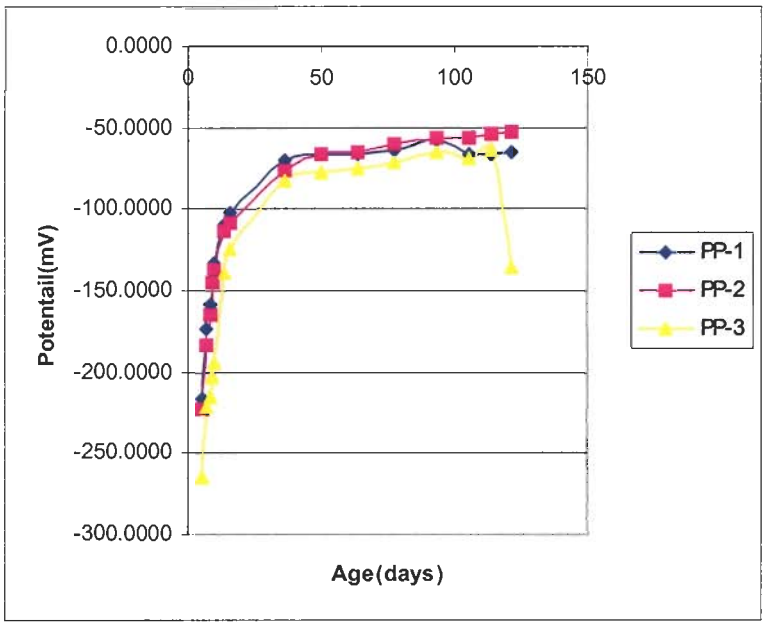


**Figure 28. Open-Circuit Potential versus Age for PP Concrete Cylinders Exposed to Sea Water**

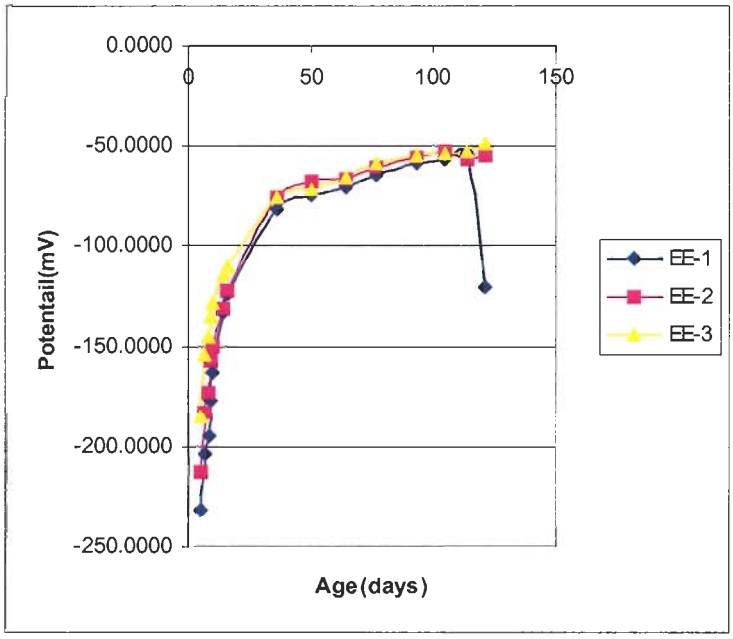


**Figure 29. Open-Circuit Potential versus Age for EE Concrete Cylinders Exposed to Sea Water**

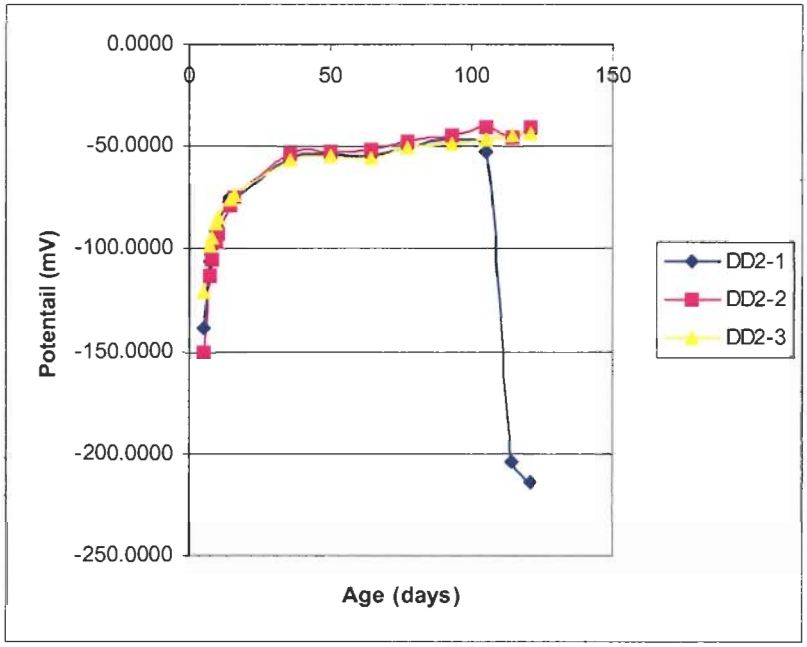


**Figure 30. Open-Circuit Potential versus Age for DD2 Concrete Cylinders Exposed to Sea Water**

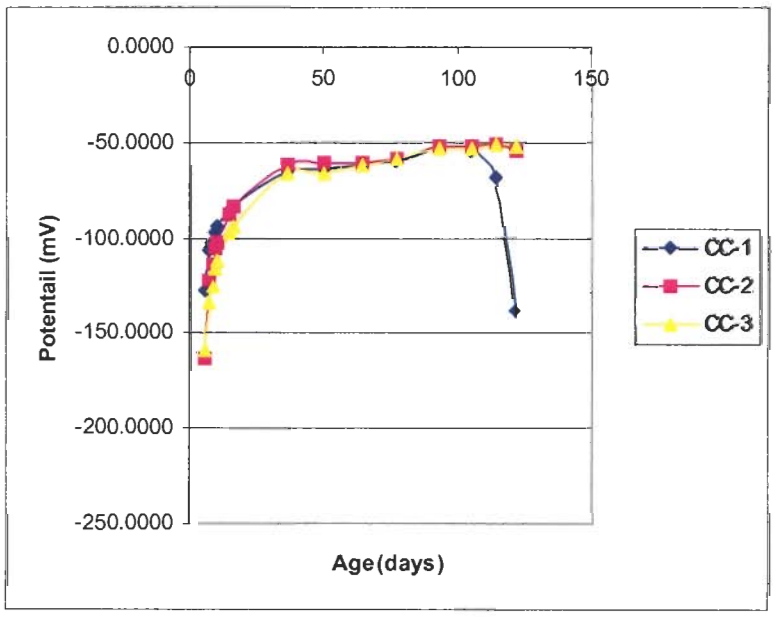


**Figure 31. Open-Circuit Potential versus Age for CC Concrete Cylinders Exposed to Sea Water**

## 3.3 Microscopic Assessment of Deterioration

From the data presented in this study, it is evident that tricalcium silicate content affects durability of concrete materials. Microstructural analysis using x-ray diffraction and scanning microscopy were used in order to assess the structural changes accompanying paste deterioration. Diffraction patterns collected from mortar bars at the end of exposure time to sodium sulfate solution revealed high ettringite and gypsum contents. The results, presented in Figure 32, indicate that as tricalcium silicate content of the as-received cement increases, there is a matching increase in the amount of ettringite and gypsum present in the paste microstructure. Increasing tricalcium silicate content of the cement results in an increase in the calcium hydroxide content which then becomes available for gypsum and ettringite formation. The presence of lime is known to affect the expansion behavior of ettringite.

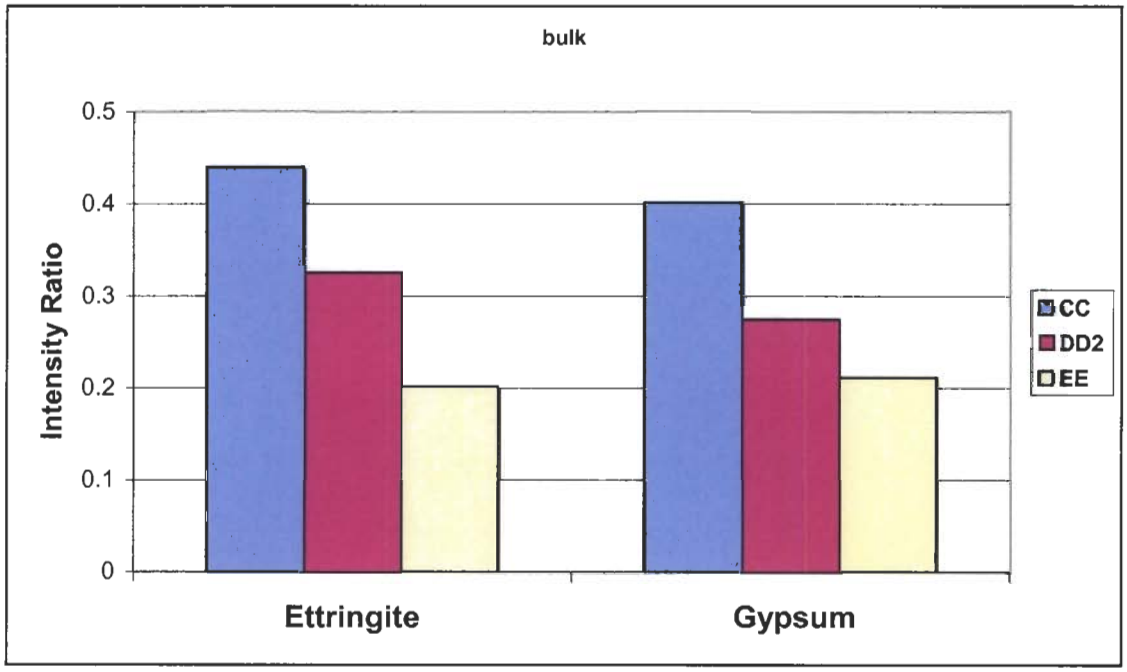


**Figure 32. Phase Abundance in Deteriorated Paste Exposed to Sodium Sulfate Solution**

The same observation was made for cements doped with lab prepared alite. This can be seen in Figure 33, where results for PPD cement are depicted. For purposes of

comparison, PP cement is also included. It is to be noticed that the data was collected for PPD cement at an age of 160 days when the mortar bar disintegrated to pieces at a corresponding expansion of about 2%. The data collected for the PP specimen was at an age of 240 days. The bar surface was used for this analysis as opposed to the bulk. The abundance of ettringite and gypsum on the outer surface of PPD is very clear.

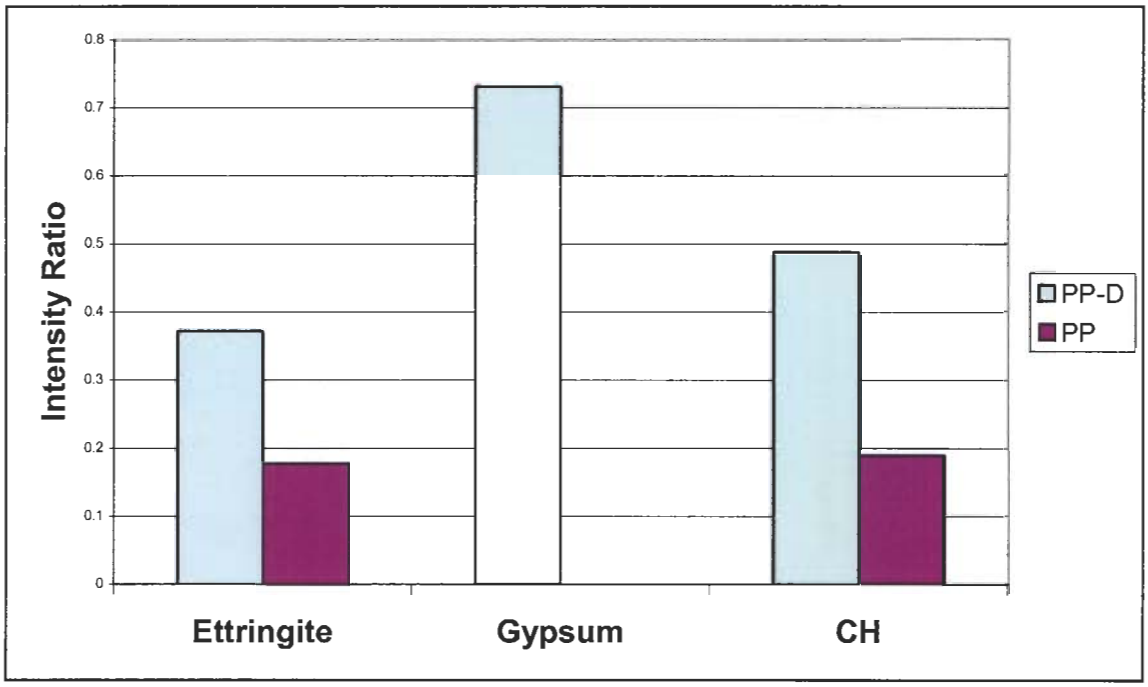


**Figure 33. Phase Abundance in Deteriorated Bars of PP and PPD Cements**

Scanning microscopy confirmed two morphologies for ettringite as shown in Figure 34 for PP cement and Figure 35 for PPD cement. For specimens that experienced excessive expansion as PPD, ettringite had very fine, slender prismatic crystals. These fine ettringite crystals have a size development affected by high CH concentrations. While in other samples ettringite crystals were disjointed, forming only local clusters, in PPD ettringite crystals seemed to form an interconnected web of crystals that covered the whole sample. In PP cement, ettringite formations were larger in size as shown in Figure 34. Similar observations were reported by others [25].

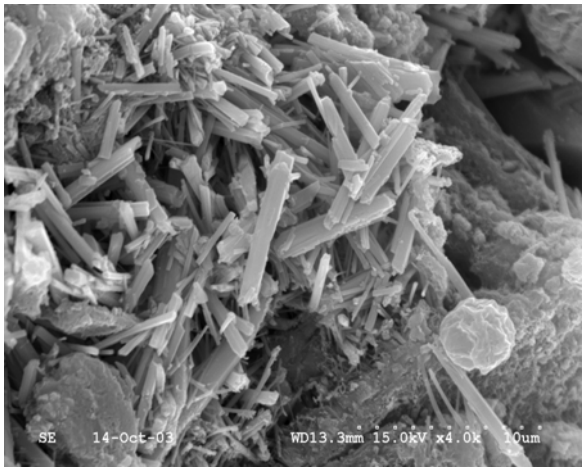


**Figure 34. Ettringite Appearance in PP Cement**

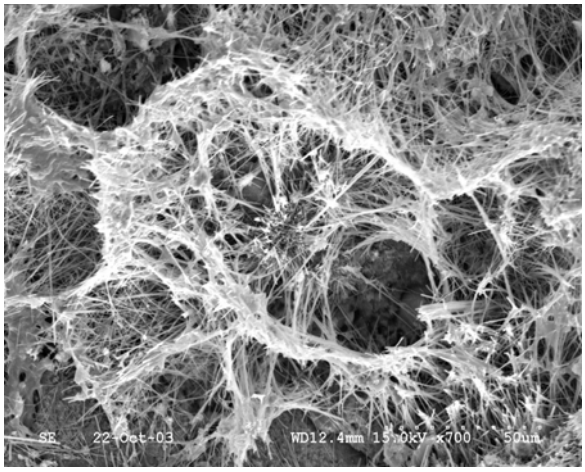


**Figure 35. Ettringite Morphology in PPD Cement**

# CHAPTER IV
# CONCLUSIONS AND RECOMMENDATIONS

The following is a summary of the findings of this investigation on the effect of tricalcium silicate on structural durability:

1. Tricalcium silicate content affects the rate and the amount of strength loss for mortar specimens exposed to sulfate environment. A drop of 1,500 psi was reported at 120 days for mortars that contained cements with tricalcium silicate content of 69% (Bogue calculations).
2. Tricalcalcium silicate content affects the rate and magnitude of expansion for specimens exposed to sodium sulfate solution. Levels of expansion of 1.0% were reported for calcium silicate content of 60% (Bogue calculations) at an age of 330 days.
3. For cements with similar tricalcium aluminate content, bars prepared with cements with tricalcium silicate content of 57% experienced significantly lower expanion. Expansion reported for those specimens was approximately 0.18%.
4. RCP measurements showed a strong correlation with tricalcium silicate content. Increasing tricalcium silicate content above 57% (Bogue calculations) increased the rate of charge passage from moderate to high.
5. OCP measurements for the period reported here did not statistically depend on tricalcium silicate content.
6. Concrete cylinders made with high C3S cements (above 57% Bogue estimate) and exposed to sulfate environments, experienced leveling off or drop in strength at an early age of 120.

The following is the suggested recommendation based on the findings of this study:

1. In order to maintain durability of structural concrete in sulfate environments, a maximum limit on tricalcium silicate content of portland cement has to be in effect.

## REFERENCES


1. Hewlett, Peter C, ed. (1998). *Lea's Chemistry of Cement and Concrete, 4th ed.* John Wiley & Sons, Inc., New York, NY.
2. Mindess, Sidney and Young, J. Francis. (1981). *Concrete.* Prentice-Hall, Inc., Englewood Cliffs, NJ.
3. Taylor, H. F. W. (1997*). Cement Chemistry, 2nd ed*. Thomas Telford Publishing, London, UK.
4. Taylor, J. C., Hinczak, I., Matulis, C. E. (2000). "Rietveld Full-Profile Quantification of Portland Cement Clinker: The Importance of Including a Full Crystallography of the Major Phase Polymorphs." *Powder Diffraction*, Vol. 15, No. 1, pp. 7-18.
5. Skalny, J., Marchand, J, Odler, I. (2002). *Sulfate Attack on Concrete.* Spon Press, New York, NY
6. Deng, M., Tang, M. (1994). "Formation and Expansion of Ettringite Crystals." *Cement and Concrete Research*, Vol.24, pp. 119-126
7. Mehta, P. K. (1973). "Mechanism of Expansion Associated with Ettringite Formation". *Cement and Concrete Research*, Vol. 3, pp.1-6.
8. Yang, S., Zhongzi, X., and Mingshu, T. (1996). "A Reply to Discussion by B. Mather of the Paper "The Process of Sulfate Attack on Cement Mortars." *Advanced Cement Based Materials*, Vol. 5, pp. 111-112.
9. Odler, I., Wonnemann, R. (1983). "Effect of Alkalies on Portland Cement Hydration: I. Alkali Oxides Incorporated into the Crystalline Lattice of Clinker Minerals." *Cement and Concrete Research*, Vol. 13, pp.477-482
10. Odler, I., Wonnemann, R. (1983). "Effect of Alkalies on Portland Cement Hydration: II. Alkalies Present in Form of Sulfates." *Cement and Concrete Research*, Vol. 13, pp.771-777.
11. Yang, S., Zhongzi, X., and Mingshu, T. (1996). "The Process of Sulfate Attack on Cement Mortars." *Advanced Cement Based Materials*, Vol. 4, pp. 1-5.

12. Tian, B., Cohen, M. D. (2000). "Expansion of Alite Paste Caused by Gypsum Formation during Sulfate Attack." *Journal of Materials in Civil Engineering*. February 2000, pp. 24-25.
13. Mindess, S., Young, J.F. (1981). *Concrete.* Prentice-Hall, Inc., Englewood Cliffs, N.J., pp. 548-551.
14. Santhanam, M., Cohen, M. D., Olek, J. (2002) "Mechanism of Sulfate Attack: A Fresh Look. Part 1: Summary of Experimental Results." *Cement and Concrete Research*, Vol. 32, pp. 915-921
15. Tian, B., and Cohen, M. D. (2000). "Does Gypsum Formation during Sulfate Attack on Concrete Lead to Expansion?" *Cement and Concrete Research*, 30, pp. 117-123.
16. Irassar, E. F., González, M., and Rahhal, V. (2000). "Sulfate Resistance of Type V Cements with Limestone Filler and Natural Pozzolana." *Cement and Concrete Composites*, Vol. 22, pp. 361-368.
17. Tian, B., Cohen, M. D. (2000). "Expansion of Alite Paste Caused by Gypsum Formation during Sulfate Attack." *Journal of Materials in Civil Engineering*. February 2000, pp. 24-25Gonzalez, M. A., and Irassar E. F. (1997). "Ettringite Formation in Low $C_3A$ Portland Cement Exposed to Sodium Sulfate Solution." *Cement and Concrete Research*, Vol.27, pp. 1061-1072.
18. Cao, H. T., Bucea, L., Ray, A., Yozghatlian, S. (1997). "The Effect of Cement Composition and pH of Environment on Sulfate Resistance of Portland Cements and Blended Cements." *Cement and Concrete Composites*, Vol.19, pp. 161-171.
19. Arenes-Oliva, G. A. *Influence of the Variation of Cement Source on Fresh and Hardened Concrete Properties*. Master's Thesis, University of South Florida, May 2002.
20. Jenkins, R., Snyder, R. L. (1996). *Introduction to X-ray Powder Diffraction.* John Wiley & Sons, Inc., New York, NY.
21. Taylor, J. C., Hinczak, I., Matulis, C. E. (2000). "Rietveld Full-Profile Quantification of Portland Cement Clinker: The Importance of Including a Full Crystallography of the Major Phase Polymorphs." *Powder Diffraction*, Vol. 15, No. 1, pp. 7-18.

22. Courtial, M., de Noirfontaine, M. -N., Gasecki, G., Signes-Frehel, M. (2003). "Polymorphism of Tricalcium Silicate in Portland Cement: A Fast Visual Identification of Structure and Superstructure." *Powder Diffraction*, Vol. 18, No. 1, pp. 7-15.
23. Nishi, F., Takeuchi, Y., Maki, I. (1985). "Tricalcium silicate, $Ca_3O(SiO_4)$: The Monoclinic Superstructure." *Zeitschrift Fur Kristallographie*, Vol. 172, No. 3-4, pp. 297-314.
24. Mumme, W. G. (1995). "Crystal Structure of Tricalcium Silicate from a Portland Cement Clinker and Its Application to Quantitative XRD Analysis." *Neues Jahrbuch Fur Mineralogie-Monatshefte*, No. 4, pp. 145-160.
25. Famy, C., Taylor, H. F. W. (2001). "Ettringite in Hydration of Portland Cement Concrete and Its Occurrence in Mature Concretes." *ACI Materials Journal*, Vol. 98, No. 4, pp. 350-356.